Phonon related properties of transition metals, their carbides, and nitrides: A first-principles study

E. I. Isaev[a)]
Condensed Matter Theory Group, Physics Department, Uppsala University, S-751 21 Uppsala, Sweden and Theoretical Physics Department, Moscow State Institute of Steel and Alloys (Technological University), 4 Leninskii prospect, Moscow 117049, Russia

S. I. Simak and I. A. Abrikosov
Department of Physics, Chemistry and Biology (IFM), Linköping University, SE-581 83 Linköping, Sweden

R. Ahuja
Condensed Matter Theory Group, Physics Department, Uppsala University, S-751 21 Uppsala, Sweden

Yu. Kh. Vekilov
Theoretical Physics Department, Moscow State Institute of Steel and Alloys (Technological University), 4 Leninskii prospect, Moscow 117049, Russia

M. I. Katsnelson
Institute for Molecules and Materials, Radboud University of Nijmegen, NL-6525 ED Nijmegen, The Netherlands

A. I. Lichtenstein
International Institut für Theoretische Physik, Universitaet Hamburg, Jungiusstrasse 9, 20355 Hamburg, Germany

B. Johansson
Condensed Matter Theory Group, Physics Department, Uppsala University, S-751 21 Uppsala, Sweden and Applied Materials Physics, Materials Science Department, The Royal Technological University, SE-100 44 Stockholm, Sweden

(Received 12 March 2007; accepted 30 April 2007; published online 25 June 2007)

Lattice dynamics of body-centered cubic (bcc) V^b-VI^b group transition metals (TM), and $B1$-type monocarbides and mononitrides of III^b-VI^b transition metals are studied by means of first-principles density functional perturbation theory, ultra soft pseudopotentials, and generalized gradient approximation to the exchange-correlation functional. Ground state parameters of transition metals and their compounds are correctly reproduced with the generated ultrasoft pseudopotentials. The calculated phonon spectra of the bcc metals are in excellent agreement with results of inelastic neutron scattering experiments. We show that the superconductivity of transition metal carbides (TMC) and transition metal nitrides (TMN) is related to peculiarities of the phonon spectra, and the anomalies of the spectra are connected to the number of valence electrons in crystals. The calculated electron-phonon interaction constants for TM, TMC, and TMN are in excellent agreement with experimentally determined values. Phonon spectra for a number of monocarbides and mononitrides of transition metals within the cubic NaCl- and hexagonal WC-type structures are predicted. Ideal stoichiometric $B1$ crystals of ScC, YC, and VC are predicted to be dynamically stable and superconducting materials. We also conclude that YN is a semiconductor. © *2007 American Institute of Physics*. [DOI: 10.1063/1.2747230]

I. INTRODUCTION

Transition metal (TM) carbides (TMC) and nitrides (TMN) are metallic compounds with outstanding physical properties, e.g., they are extremely hard, and their melting temperature is very high. For instance, the melting temperature (about 4200 °C) of TaC is the highest among known materials. Besides, TMC, as well as TMN, are chemically very stable and have high corrosion resistance. Due to these circumstances, they are widely used in the industry, e.g., as cutting tools. They have also potential applications in, for example, information storage technology (for coating of magnetic sheets), high power energy industry, and optoelectronics.

Besides a number of exciting physical properties, they also adopt several crystal structures. It is well known that TMC and TMN can crystallize in different crystal lattices and form different phases, depending on the R_X/R_M ratio where R_M and R_X are the atomic radii of metallic and nonmetallic atoms, respectively. They form simple crystal structures with MX, M_2X, M_4X, and MX_2 stoichiometries, if Hägg's rule, $R_X/R_M < 0.59$,[1] is fulfilled. In practice, the phases are not stoichiometric and they exist over a wide concentration range. Carbides and nitrides of TMs with the MX stoichiometry are usually cubic, where the metallic atoms

[a)]Electronic mails: eyvaz_isaev@yahoo.com and Eyvaz.Isaev@fysik.uu.se

form the face-centered cubic (fcc) sublattice, and nonmetallic atoms occupy interstitial positions, forming NaCl-type structure, for example, ZrC, TiC, NbC, TiN, and ZrN.[2,3] Unusual physical properties (extremely high melting temperature, brittleness, and conductivity) suggest that the atomic bonding between metallic and nonmetallic atoms in carbides and nitrides of TMs is very strong, and has a covalent nature. As a matter of fact, TiC has metallic conductivity character, but some nitrides, ScN as example, appear to be semiconductor.

The physical and thermodynamical properties of TM carbides and nitrides have been well reviewed in Refs. 2 and 3. Their electronic properties have been studied by means of both experimental and theoretical methods, and the general trends as a function of composition and TM atom type are summarized in Ref. 4. A review of lattice dynamics properties of TMs and their compounds has been given in Ref. 5. The density of electronic states (DOS) of TiC, TiN, and TiO was studied by means of the linear combination of atomic orbitals (LCAO) and the augmented plane wave (APW) methods, and the role of covalent metal-nonmetal interaction in structural stabilization of the compounds has been emphasized.[6–8] Electronic structure, DOS, and optical properties of monocarbides, -nitrides, and -oxides of Ti and Zr have been investigated in Refs. 9 and 10 using the full-potential linear muffin-tin orbital (FP-LMTO) method. Electronic band structure of NbC (Refs. 11–13) and NbN (Refs. 11–14) was examined by means of the APW, full-potential linearized augmented plane wave (FP-LAPW), and pseudopotential methods. It has been shown that the conduction electrons in NbN have mainly 4*d*-like character and NbC and NbN are *d*-type superconductors. It has been confirmed by nuclear spin-lattice relaxation time measurements.[15] The electronic structure and physical properties of early transition metal carbides and nitrides in the $B1$ structure have been studied by means of the LMTO and FP-LAPW methods, as well as in the framework of *ab initio* pseudopotential techniques.[16–19] It has been reported that in comparison with the local density approximation (LDA), the use of the generalized gradient approximation (GGA) improves the agreement with experiment. Besides, band structure calculations performed by means of the screened-exchange LDA method have shown that some of the nitrides (ScN, YN, and LaN) have semiconducting nature with indirect band gaps, comparable with those for conventional semiconductors. Electronic properties of some transition metal nitrides (VN, NbN, TaN, CrN, MoN, and WN) with the $B1$ structure have been studied[20] using the APW method. Earlier studies[21,22] of NbN and MoN showed an unusual increase of the DOS of MoN in comparison with NbN, which is known to be a superconductor with high T_c [14.7 K,(Ref. 23) or even 20 K (Ref. 24)]. The predicted value of T_c was about 30 K, close to T_c of the first copper oxide based superconductors and MgB_2.[25] The same temperature, 30 K, was predicted theoretically for VN, but it was believed that spin fluctuatioins should be responsible for the reduced experimental value $T_c \approx 8.6$ K.[26] Besides, it has been found that though the DOS of CrN is larger than that of MoN, the contribution to the electron-phonon coupling arising from a metal is small in CrN.

Jhi *et al.*[27] using the first-principles pseudopotential method have studied the influence of vacancies on mechanical properties of TM carbides and nitrides, something which turned out to be different for carbon and nitrogen vacancies. Carbon vacancies result in hardening of the host matrix, whereas nitrogen vacancies lead to softening of the shear elastic stiffness due to the opposite way in filling of the *d-d* bonding states at the Fermi level, i.e., the DOS from *dd* states is reduced for NbC, and increased for TiN. Mechanical properties (such as elastic constants, hardness, Young's and shear moduli, and the equation of state) of HfN, ZrN, and NbN were examined experimentally, as well as theoretically[28,29] using *ab initio* pseudopotentials and the linear response of the unperturbed system to homogeneous strains developed by Hamann *et al.*[30] The different behavior of the bulk moduli B, tetragonal shear G', and shear moduli G for TMN and TMN was explained in terms of band filling. The observed relationship between the elastic constants ($C_{11} > C_{44} > C_{12}$) for HfN and ZrN determined from neutron scattering experiments is not obeyed for NbN. Tetragonal shear moduli G for transition metal carbonitrides, $MeC_{1-x}N_x$, and di-transition-metal carbides, $A_{1-x}B_xC$ is considerably enhanced for a valence electron number of $Z_v = 8.3$.

The nature of metal-to-insulator transition in $B1$ TaN_x and the role of Ta and N vacancies was studied experimentally, as well as by means of the first-principles FLAPW method.[31,32] It was shown that the conductivity of TaN_x can be tuned by means of the N_2 pressure, as well as by temperature. In turn, the conductivity for N-rich Ta–N system, as a consequence, the metal-insulator transition, is mainly connected to Ta vacancy and/or Ta-poor regions in the system. The influence of nonmetal off stoichiometry, as well as substitutional impurities, on the phase stability and thermodynamics properties in MoC_x and TiC_x alloys is discussed in Ref. 33.

Experimental investigations of the phonon spectra of TM carbides (NbC, HfC, and TaC) have been done by Smith and co-worker[34–36] where pronounced anomalous of the phonon dispersion curves along the [100] and [110] directions for NbC and TaC were found, while the spectrum for HfC did not contain any anomalies. This was used by these authors to explain why TaC is a superconductor, while HfC is not, at least, for $T > 1$ K,[34] even though Hf and Ta are both refractory metals with closely related physical properties.

Mostoller[37] carried out phonon calculations for TM carbides in the framework of the dielectric response approximation using the Heine-Abarenkov pseudopotentials.[38] It is amazing that the calculated acoustic branches of the phonon spectrum for uranium carbide (UC) are in fairly good agreement with the results of experiment.[36] However, the model was not able to reproduce the observed anomalies of the phonon dispersion curves for HfC, TaC, and NbC near the Brillouin zone (BZ) boundaries. It was claimed that including of the ion-ion interaction neglected in these calculations could lead to a better agreement between theoretical and experimental results. Pintschovius *et al.* applied inelastic neutron scattering to study the phonon dispersion relations in TiC.[39] They also studied the influence of carbon vacancies on the spectrum. It was found that the largest difference between the spectra for $TiC_{0.95}$ and $TiC_{0.89}$ was about 3.5% and

that it is mainly the optical modes which are affected by carbon vacancies. The influence of carbon vacancies on the first-order Raman spectrum of TiC was investigated in Ref. 40. The measured spectrum for TiC,[39] as well as the phonon spectra for a number of TM carbides (ZrC, NbC, TaC, HfC, and UC), have been examined by means of the phenomenological "double-shell" model[41] (DSM) (in this model *d* electrons are represented by a second shell at the TM atoms, and the first shell describes the polarizability of all the other valence electrons; besides, it was suggested that springs between the second shells are negative), where long-range order interatomic interactions were taken into account because the simple shell model did not give a good agreement with the experimental dispersion curves. The connection between phonon anomalies and high superconducting temperature T_c, as well as electron-phonon coupling constants in TM carbides and nitrides, was studied by Weber and co-workers in Refs. 42 and 43 using the strong coupling theory of superconductivity.[44,45] They suggested a "resonant electronic polarization" model (this leads to a phonon softening and is tightly related to the DSM, where in certain regions of the BZ negative springs between second shells compensate the positive core-shell coupling constant leading to resonantlike enhancement of the electronic polarizability in these BZ regions) and, as a result, concluded that the electron-phonon matrix elements are mainly determined by strong *d-d* overlap interaction. Sinha and Harmon,[46] using the dielectric function, have shown that the self-consistent field theory predicts a collective electron instability due to the charge fluctuation between the *d* shells. However, the instability is prevented by the electron-phonon interaction, though the interaction might result in an anomaly in the phonon spectrum. The model was applied to NbC and peculiarities of the calculated phonon spectra were found to be in fairly good agreement with the experimental results of Smith and Gläzer.[36] The role of three-body interactions was emphasized for the lattice dynamics of TiC, ZrC, and HfC when investigated in the rigid shell model.[47]

Ab initio phonon calculation for a TM carbide (NbC) has been done by Savrasov[48] using the linear response technique in the framework of the LMTO. The agreement between theory and experiment was fairly good. The peculiarities of the spectrum along the $[\xi 00]$ direction [near the $2\pi/a(0.6,0,0)$ point] were well reproduced, while anomalies along the high symmetry $[\xi,\xi,0]$ direction were not so pronounced compared to the model calculations of Weber.[41] This discrepancy was attributed to the small number of $\mathbf{q}$ points for which the spectum was calculated and then used for interpolation of the phonon spectrum for a given direction. At high pressure the superconducting temperature of NbC is suppressed down to 4.9 K at 60 GPa, and as low as ~1 K at 150 GPa,[49] to be compared with 11.2 K at ambient pressure.[43] First-principles investigation of the phonon spectrum for TiC (Ref. 50) and ZrC (Ref. 51) have been done in the framework of the supercell method, and the Hellmann-Feynman force theorem in conjunction with norm-conserving pseudopotentials was applied to calculate interatomic force constants. The phonon dispersion curves and density of states were calculated and good agreement between theory and experiment was found, though it was achieved by reducing the calculated spectra by a factor of 1.05. Besides, there was a considerable discrepancy between the calculated elastic constants, especially for C_{12}, and the ones from ultrasonic experiments. This discrepancy was ascribed to the difference in slope of the experimental and theoretical phonon dispersions near the BZ center which is, presumably, caused by lacking some of the force constants required for the description of the long-range Coulomb interaction.

Anomalies of the phonon spectrum in TiN and ZrN show a dip of the LA mode at $\mathbf{q}\approx 2\pi/a(0.7,0,0)$ and $\mathbf{q}\approx 2\pi/a(0.5,0.5,0)$ points, as well as softening of the LA mode near the *L* point, has been observed experimentally in Refs. 52 and 53, and the results are well described using the phenomenological DSM. The isoelectronic HfN possesses the same anomalies[54] for the acoustic branches, but in HfN, in contrast to other TM carbides and nitrides, a so-called inversion of the longitudinal optic (LO) and transversal optic (TO) branches takes place where the TO modes are higher in energy than the LO branch. It turned out that there is a strong influence of nitrogen vacancies on the Raman spectrum, phonon density of states and, consequently, superconductivity of TiN_{1-x} compounds.[55] Inelastic-neutron-scattering measurements[56,128] revealed that acoustic branches of the phonon spectrum of VN are completely different compared to TiN and NbC, and the anomalies of the spectra are shifted to the *X* point of the BZ, while for other carbides and nitrides with the *B*1 structure the special features of the spectra are located near the point $2\pi/a(q,0,0)$ along the high symmetry Δ direction where $q\approx 0.65-0.70$. Tunneling measurements for VN have been done in Ref. 57 where the Eliashberg spectral function $\alpha^2F(\omega)$ for VN was found to be similar to that of NbN for which optical phonons are believed to play an important role for superconductivity. Physical propertes of some TM compounds including TMC and TMN have been studied in Ref. 58. The relation between lattice instabilities and high values of the superconducting temperature T_c in TM and their compounds was established by Phillips,[59] Frölich,[60] and Zeller.[61] Pressure induced changes in the phonon spectrum, as well as in the electron-phonon coupling, superconducting temperature, and the Debye temperature were studied using Raman-scattering measurements.[62] Applying high pressure up to 32 GPa resulted in a shift of the phonon DOS, and the phonon spectrum accordingly, to higher frequences (the so called pressure-induced phonon hardening). T_c for HfN and ZrN is decreased with increased pressure (as it was observed for most conventional metals), while for NbN an increase of T_c on compression is observed. The phonon spectrum and electron-phonon coupling constants for ZrN and HfN at ambient conditions have been calculated[63] based on the mixed-basis pseudopotential and linear response methods. Nevertheless, it is worth noting that the phonon spectra for most of the TM nitrides are not yet investigated theoretically using first-principles methods and the study of the phonon dispersion relations in TMN is one of the tasks of the present work.

Another interesting fact is that some of the transition metal monocarbides and mononitrides have never been syn-

thesized experimentally in the cubic $B1$ structure, for example, MoC and MoN. This unusual behavior is ascribed, but just schematically, to the phonon instability at the X point.[64] Recently, $B1$ MoN was found to be unstable, because the calculated elastic modulus C_{44} turned out to be negative.[29]

There is a large body of theoretical and experimental studies, where electronic,[65] surface-related properties,[66] as well as phonon modes,[67] caused by violated Bloch periodicity, have been investigated for a number of carbides and nitrides. In this work we do not consider surface phonon dispersion relations in the TMC and TMN. They are the subject of our future studies.

In our previous communication we studied the phonon spectra, as well as the electron-phonon coupling constant λ for selected TMC and TMN.[68] In the present paper we investigate the ground state properties and phonon spectra of all the III^b-VI^b metal carbides and nitrides, except those with La and Cr, for which only lattice parameters and bulk moduli are presented. It is well known that chromium carbide has a rather complex structure and that $B1$ CrC was synthesized recently.[69] Chromium nitride was also produced recently, and there is some controversial information concerning the CrN lattice structure. In particular, an antiferromagnetic phase was found for almost stoichiometric CrN.[70,71] There are only few publications devoted to LaC (Ref. 16) and LaN.[16,17,72] Besides, there is no experimental information on the lattice dynamics of LaC and LaN. Investigation of the dynamic stability of different phases of La and Cr carbides and nitrides is in progress, and the results will be reported elsewhere. We have also studied electron-phonon coupling constants of the III^b group metals, and TM carbides and nitrides containing seven and nine valence electrons in the unit cell.

The paper is organized as follows. In Sec. II we describe the details of ultrasoft pseudopotential generation, the calculations of the total energy, and phonon spectra. In Sec. III results of first-principles calculations of lattice constants and bulk moduli for selected bcc metals and all considered TMC and TMN are presented and compared to available experimental and theoretical results. In Sec. IV we discuss the phonon spectra for bcc transition metals illustrating good performance of the generated ultrasoft pseudopotentials. The main results for the phonon spectra of TMC and TMN are described in Sec. V. Section VI is devoted to a discussion of the obtained results and to some general conclusions. In this section the calculated electron-phonon coupling constants are also presented and compared with experimental and other theoretical results.

II. METHODS AND DETAILS OF CALCULATIONS

Our present investigation of ground state properties (lattice constant and bulk modulus) of early TMs, as well as their carbides and nitrides, is done in the framework of the density functional theory[73,74] within the state-of-the-art first-principles ultrasoft (US) pseudopotential method introduced by Vanderbilt.[75] Exchange-correlation effects were treated in the framework of the generalized gradient approximation (GGA) using a functional proposed by Perdew-Burke-Ernzerhof,[76] which was found to reproduce correctly ground state parameters for a wide range of crystals. For Cr, CrC, and CrN we, however, applied Becke-Perdew exchange-correlation functional,[77] known to correctly describe the magnetic structure of Cr.

The neutral atomic configurations were chosen to be the reference state. Only for Ti and Zr the reference state was chosen to be a single charged metal ion. Semicore orbitals were considered as valence states for all III^b-VI^b metals (excluding La and Cr), and nonlinear core corrections[78] are also included. Besides, the d channel was treated as the local part of the pseudopotential. A scalar-relativistic version of the Schrödinger equation was applied in order to get atomic wave functions to be used for the pseudopotential construction.

For La, Hf, Ta, and W the $4f$ state is not considered as a valence state, because it is completely filled (14 electrons) and is chemically inert. The same approach was used in Ref. 79 for the investigation of the phonon spectra of lanthanum by means of a first-principles pseudopotential method in conjunction with the frozen-phonon method. The obtained results gave rise to the conclusion that the assumption worked well and that anomalies of the phonon spectra of fcc La are not connected to the $4f$ electrons.

Plane waves (PWs) with cutoff energy up to 40 Ry were used in order to describe the electronic wave functions in a periodic crystal, and PWs up to 750 Ry were included for description of the augmented charge. Integration over the BZ has been done using the Monkhorst-Pack scheme,[80] and occupation numbers are treated according to the Methfessel-Paxton scheme[81] with a broadening $\sigma=0.025$ Ry using the first-order Hermite-Gauss type of polynomial. Integration over the BZ was carried out using an $18\times18\times18$ mesh of k points.

The lattice dynamics of the present systems of interest was studied in the framework of the harmonic approximation to the force constants and using the linear response method[82] which is realized in the Quantum ESPRESSO code.[83] In this method the response of a system to the atomic displacements is a linear function of parameters and their first-order derivatives which are defined in terms of parameters (charge density, electron-ion interation, and exchange-correlation functional) of the unperturbated system [so-called density functional perturbation theory (DFPT), see Ref. 82]. The method allows one to avoid a need for a supercell construction, so all calculations are done within a single unit cell. The method enables calculation of the phonon frequencies for an arbitrary $\mathbf{q}$ point in the BZ using force constant matrices for a given $\mathbf{q}$ point mesh and inverse Fourier transformation to obtain real-space force constants. As a matter of fact, the knowledge of the phonon spectrum makes it possible to draw some conclusions about the physical properties of a crystal. For example, the appearence of imaginary frequences is a strong argument for lattice instability and therefore, for a phase transformation. Peculiarities (a dip and softening of acoustic modes) of the spectrum are also often precursors for phase transformations and could be related to the onset of superconductivity in the crystal.

In order to derive the detailed account of peculiarities of

the acoustic modes, force constant calculations are performed using an $8\times8\times8$ **q** mesh in the case of $B1$ TMC and TMN, as well as for the bcc metals, and an $4\times4\times4$ **q** grid for hexagonal monocarbides and mononitrides (MoC, NbN, WC, and WN). The electron-phonon coupling constant λ is calculated in the framework of strong-coupled superconductivity theory of Eliashberg[45] using an $8\times8\times8$ **q** mesh for the bcc metals and $6\times6\times6$ **q** mesh for the carbides and nitrides with seven and nine electrons in the unit cell. The superconducting temperature is evaluated by means of McMillan's equation[44] modified by Allen and Dynes[84] where a logarithmic frequency was introduced instead of the empirical Debye temperature.

III. GROUND STATE PROPERTIES OF BCC METALS, AND TM CARBIDES AND NITRIDES

In order to investigate the transferability of TMs' pseudopotentials, we have calculated the ground state properties for TM carbides and nitrides, as well as for bcc metals (V, Nb, Ta, Mo, and W). Results are summarized in Tables I–III and compared with available experiments and results of other calculations. The equilibrium lattice constants and bulk moduli are obtained from the total energy calculated for a given number of lattice parameters, followed by the fitting of these results to the Birch-Murnaghan equation.[85]

Let us analyze the ground state parameters of pure bcc (V, Nb, Cr, Ta, Mo, and W), double hexagonal close packed (DHCP) La, and hexagonal close packed (HCP) metals (Y, Sc, Ti, Zr), see Table I. One can see that for the bcc metals there is a very good agreement, better than 1%, between the calculated and experimental lattice parameters. Most of the calculated bulk moduli agree with experimental data and first-principles calculations[86] within 6%, excluding V, for which the disagreement with experiment[87] is of about 10%. The discrepancy may mean that the cut-off radii for V should be chosen more carefully. As a matter of fact, parameters for the vanadium pseudopotential were chosen to get acoustic frequencies close to zero at the Γ point, so that the acoustic sum rule is approximately fulfiled. We have applied the same procedure for other bcc metals and found that the agreement of the obtained lattice parameters and bulk moduli with available data is much better compared to V. On the other hand, the experimental bulk modulus provided in Ref. 4 is 172 GPa which agrees well with our calculated value. For DHCP La the calculated **c** paramater is somewhat larger than the experimental value,[87] but the difference is less than 1%. As a result, calculated bulk modulus for DHCP La is in good agreement with the experimental one. Overall agreement for both lattice parameters and bulk moduli for the HCP metals is very good, except for Zr, for which the calculated bulk modulus is by ~13% larger than the old experimental values for B.[87,88] Indeed, the calculated B turned out to be in excellent agreement with recent results of synchrotron x-ray experiments.[89] It is worth noting that for Cr a pseudopotential used in this work yielded not only a good agreement for the lattice parameter and bulk modulus, but it also allowed us to describe correctly the magnetic moments of atomic force microscopy (AFM) Cr, $0.67\mu_B$, in good agreement with experimental observations.[90] Note also that the use of the PAW+GGA approximation resulted[91] in a large local magnetic moment for Cr atoms, of order of $1\mu_B$, and in a smaller lattice parameter (2.85 Å) while calculated B was consistent with the reported experimental data.

TABLE I. Ground state parameters for bcc (V, Nb, Ta, Cr, Mo, and W), DHCP (La), and HCP (Y, Sc, Ti, Zr, and Hf) metals using ultrasoft pseudopotentials generated in this work. For each metal first we show results of our calculations, and on the next line available experimental (Ref. 87 if nothing specified) and theoretical data are presented.

Metal	a (Å)	c (Å)	B (GPa)
V	2.995		182
	3.03		161, 172[a,b]
Cr	2.871		202
	2.88		190
Nb	3.30		172
	3.30		170
Ta	3.30		194
	3.31		200, 194[c]
Mo	3.16		258
	3.15		272, 265[c]
W	3.18		303
	3.16, 320,[d] 3.16[e]		323, 314,[c] 320,[d] 274[e]
La	3.77	12.266	22
	3.77	12.159	24.3
Sc	3.317	5.168	54
	3.31	5.27	58.4
Y	3.651	5.689	40.6
	3.65	5.73	42
Ti	2.983	4.591	110
	2.95	4.65	107
Zr	3.23	5.15	94
	3.23	5.15	83, 85,[f] 92[g]
Hf	3.194	5.05	108
	3.19	5.05	109

[a]Reference 4.
[b]Reference 142, FP-LMTO+GGA.
[c]Reference 140, Expt.
[d]Reference 86, norm-conserving pseudopotential and LDA.
[e]Reference 92, pseudopotential+LDA.
[f]Reference 88, Expt.
[g]Reference 89, Expt.

In Table II we present results of our density functional theory (DFT)-GGA calculations for lattice parameters and bulk moduli for monocarbides of interest. We have found excellent agreement between our calculated and available experimental and theoretical lattice parameters for all monocarbides. Our calculated bulk modulus for TiC is in very good agreement with most of the available data. It is perhaps more interesting to note the origin of disagreement which occurs in comparison with other calculations. In Ref. 94 calculations were carried out by means of the LMTO method in combination with the atomic sphere approximation (ASA) which is not suitable for an open structure such as TiC. Jochym *et al.*[50] evaluated bulk modulus using the elastic constants

TABLE II. Equilbrium lattice parameters and bulk moduli for $B1$ TMC. For each TMC first we show calculated lattice constants and bulk moduli, and then available experimental and theoretical data are given on the next line.

TMC	a (Å)	B (GPa)
ScC	4.68	153
	4.72[a]	
YC	5.08	128
	5.11,[a] 5.076,[b] 5.195[c]	
LaC	5.434	80
	5.429[c]	
TiC	4.36	242
	4.3176,[a] 4.326,[d] 4.27,[e] 4.38,[f] 4.332[g]	239,[d] 310,[e] 267,[f] 242,[h] 233,[i] 220,[k] 394,[l] 273,[m] 286,[n] 235[o]
ZrC	4.699	222
	4.6957,[a] 4.698,[c] 4.692[g]	265,[b] 250,[p] 247,[q] 223[r]
HfC	4.651	238
	4.638,[a] 4.64,[q] 4.639[g]	263,[g] 243,[r] 291[s]
VC	4.154	304
	4.1599,[a] 4.22,[f] 4.13614, 4.10,[t] 4.17[g,d,s]	377,[d] 321[f] 348,[n] 351,[t] 304,[u] 303[v]
NbC	4.476	301
	4.47,[a] 4.470,[c] 4.471,[g] 4.45,[t]	340,[s] 331,[g] 315,[u] 302,[v] 332[s,w]
TaC	4.47	324
	4.44,[o] 4.457,[d] 4.456[g]	321,[u] 332,[i] 345,[x] 318[y]
CrC	4.10	322
	4.117,[c] 4.10,[f] 4.01,[s] 4.03[z]	333,[s] 351[f]
MoC	4.366	337
	4.278,[c] 4.42,[f] 4.33[i]	351,[t] 380[p]
WC	4.38	365
	4.266,[k] 4.38,[f] 4.221[g]	396[f]

[a]Reference 102.
[b]Reference 104, EP-LMTO+GGA.
[c]Reference 16, LMTO+LDA.
[d]Reference 94, Expt. Ref. 46.
[e]Reference 95, FP-LMTO+LDA.
[f]Reference 101, PsP+LDA.
[g]Reference 141, experiment.
[h]Reference 105, experiment.
[i]Reference 97, experiment.
[j]Reference 96, experiment.
[k]Reference 10, FP-LMTO+GGA.
[l]Reference 94, LMTO+ASA.
[m]Reference 103, FP-LAPW+GGA.
[n]Reference 100, FP-LMTO+GGA.
[o]Reference 106, experiment.
[p]Reference 64, FP-LAPW, LDA.
[q]Reference 29, LDA and DFPT.
[r]Reference 41, from DSM phonons.
[s]Reference 2, experiment.
[t]Reference 139, LAPW+LDA.
[u]Reference 98, LAPW+GGA.
[v]Reference 4, experiment.
[w]Reference 107.
[x]Reference 138, experiment.
[y]Reference 145, DFPT+GGA.
[z]Reference 137, experiment.

C_{11} and C_{12} calculated on the basis of the long wave method. They have noticed that there is a disagreement between the calculated C_{11} and C_{44} compared to both the experimental and the stress-strain-method calculations for the bulk modulus. Besides, they stressed that the discrepancy could be caused by the supercell method they used due to the lack of some long-range order interactions owing to restricted supercell size, which in turn could affect a slope of the acoustic

TABLE III. Ground state parameters for transition metal nitrides within $B1$ structure. Results of other calculations and experimental date are shown on the next line after results of our calculations.

TMN	a (Å)	B (GPa)
ScN	4.51	198
	4.505,[a] 4.501,[b] 4.543	1822, 201[c]
LaN	5.293	120
	5.321,[d] 5.295[e]	140[d]
YN	4.905	158
	4.889,[a] 4.85[d]	163[d]
TiN	4.275	264
	4.239,[a] 4.26,[d] 4.24,[f,g] 4.266,[h] 4.253,[i] 4.32,[j] 4.299[k]	286,[d] 288,[g] 280,[i] 304,[j] 326,[k] 310,[l] 318[m]
ZrN	4.583	250
	4.585,[a] 4.61,[b] 4.62,[n] 4.589[o]	264,[d] 272,[n] 285,[p] 215,[q] 285,[q,r] 277[o]
HfN	4.54	269
	4.52,[a] 4.54,[d] 4.47[n]	278,[d] 303,[n] 276,[p] 306[q,r]
VN	4.11	313
	4.136,[a] 4.12,[d] 4.14,[f,g] 4.132,[i] 4.19,[j] 4.092[k]	333,[d] 316,[i] 282,[g] 370,[k] 338,[j] 268[m]
NbN	4.41	309
	4.394,[a] 4.42,[d] 4.378,[j] 4.392,[t] 4.379[q]	317,[d] 350,[u] 354,[q,r] 292,[q] 287,[m] 354[q,r]
TaN	4.408	329
	4.33,[a] 4.42,[d] 4.385,[v] 4.397,[s] 4.3363[w]	338,[d] 372[r]
CrN	4.09	322
	4.168,[t] 4.058,[i] 4.140,[s] 4.148,[f] 4.09[j,x]	326,[i] 361[j]
MoN	4.328	327
	4.41,[j] 4.214,[t] 4.25,[j] 4.285[y]	354,[j] 390,[p] 360[y]
WN	4.35	354
	4.36,[j] 4.154,[z] 4.20[r]	394[j]

[a]Reference 102.
[b]Reference 144, experiment.
[c]Reference 18, FP-LAPW+GGA.
[d]Reference 17, FLAPW+GGA.
[e]Reference 72, experiment, at $P=0$ and $T=93$ K.
[f]Reference 71, experiment.
[g]Reference 94, LMTO+LDA.
[h]Reference 15 in Ref. 20.
[i]Reference 98, VASP+GGA.
[j]Reference 101, pseudopotentials+LDA.
[k]Reference 100, FLAPW+LDA
[l]Reference 10, FP-LMTO+GGA.
[m]Reference 133, experiment, using $B=(C_{11}+2C_{12})/3$.
[n]Reference 63, pseudopotentials+LDA.
[o]Reference 143, FPLAPW+GGA.
[p]Reference 16 in Ref. 63, experiment.
[q]Reference 28, neutron scattering experiment.
[r]Reference 29 LDA+DFPT.
[s]Reference 20, APW+LDA.
[t]Reference 16, LMTO+LDA.
[u]Reference 64, LAPW.
[v]Reference 63 in Ref. 17.
[w]Reference 136, experiment.
[x]Reference 70, pseudopotentials+LDA.
[y]Reference 107, LAPW+LDA
[z]Reference 135, experiment.

modes for the long-range waves. The FP-LMTO calculations[95,96] gave very different results due to the different exchange-correlation functional they used. For comparison, more references for TiC and TaC can be found in Ref. 97. Another noticeable difference is seen for VC, but experimental results taken from the same reference (see Ref. 41 in Ref. 94) are considerably different and, obviously, the disagreement could be ascribed to nonstoichiometry of the

experimental VC samples. Nevertheless, our calculated lattice constant and bulk modulus are in excellent agreement with *ab initio* GGA-based pseudopotential calculations of Siegel *et al.*[98] using ultrasoft pseudopotentials and all-electron APW potentials. It is also interesting that in Ref. 28 the calculated bulk modulus for NbN is quite large, 348 GPa, which is comparable with the bulk modulus of cubic boron nitride. Its further increase under pressure encouraged the authors of Ref. 28 to speculate about possible high-pressure application of NbN. However, the bulk modulus for NbN evaluated from neutron scattering experiments is only 292 GPa, in quite good agreement with our calculations. For ScC, YC, and LaC there are no available data; therefore, our calculations predict the bulk modulus for the carbides.

Note that recent high-pressure experiments have obtained a considerably lower value for bulk modulus of $VC_{0.85}$,[99] 258 GPa, and obviously C vacancies make $VC_{0.85}$ more compressible. Thus, $VC_{0.85}$ does not show the same behavior as NbC for which vacancy-induced hardening was observed. Most likely, this is due to the high C deficiency.

A comparison of lattice parameters and bulk moduli for TMN (Table III) with experimental and theoretical results shows that our GGA calculations in general are in good agreement with these data. The bulk moduli calculated by Hart and Klein,[64] as well as by Wolf *et al.*[100] are, however, higher than the ones we calculate. This is not so surprising, taking into account the fact that their calculations are done in the framework of the LDA, which usually results in a higher bulk modulus compared to the GGA treatment. At the same time, the agreement with LDA calculations combined with mixed-basis pseudopotentials of Heid *et al.*[63] is also good. Nevertheless, a general trend in dependence of bulk modulus on the lattice constant is the same as compared to Ref. 64, despite some difference obtained for the absolute values for the bulk modulus, mainly for LaN. One can see from Table III that the agreement between our results and the FP-LAPW-GGA calculations of Stampfl *et al.*[17] is excellent for both the lattice parameter and bulk moduli, but there is a strong deviation from the experimental bulk modulus obtained for nonstoichiometric VN. Lattice constants and bulk moduli calculated by Siegel *et al.*[98] by means of VASP agree nicely with our results. Though CrN is believed to prefer the AFM ordering of magnetic moments and, thus, a more complicated atomic structure, most of calculations have been done for the nonmagnetic $B1$ phase. Therefore, we follow these calculations for the sake of comparability. Calculated lattice parameter agrees well with available data, but calculated B using the LDA approximation and norm-conserving pseudopotential seems to be larger, instead of ultrasoft pseudopotential within GGA calculations.

In Fig. 1 we summarize our calculated B for all the TMC and TMN systems we have studied. There are some general trends in B we would like to point out. The first trend is that the bulk moduli of III^b-V^b metal nitrides are larger than those of the carbides. For CrC and CrN we obtained very similar bulk moduli, but for Mo and W they are somewhat larger for carbides compared to nitrides. The second trend is the increase of B for both TMC and TMN from III^b to V^b group metal. Thus, the difference between B(TMC) and B(TMN) is

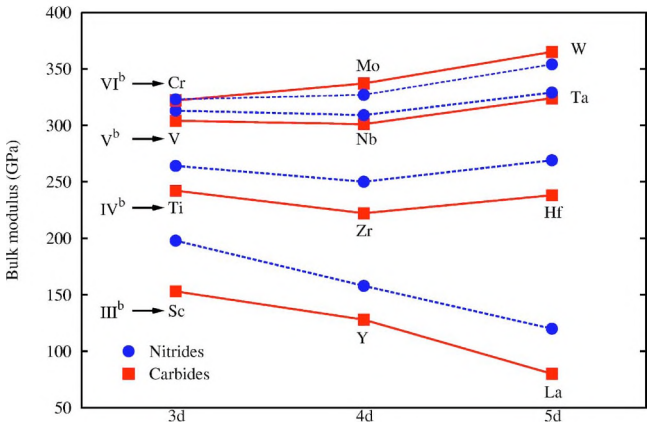

FIG. 1. (Color online) Trends in bulk moduli of III^b-VI^b group metal monocarbides and mononitrides within $B1$ structure. The filled circles refer to the carbides, and the squares stand for the nitrides.

negative for III^b-V^b metals, while it becomes positive for VI^b metal. Bulk moduli of TMC and TMN for V^b and VI^b group metals are very close to each other and, probably, they can be tuned so that they have a similar B (as an example, random $MeC_{1-x}N_x$ alloy could be considered). This might allow us to optimize the use of V^b and VI^b group TMC and TMN for practical applications. Results of *ab initio* pseudopotential calculations for a series of TMC, and TMN Ref. 101 of $3d$ and VI^b metals show similar behavior. Furthermore, we observed very unusual decrease of B for LaC and LaN. Calculated B is about 80 GPa, and 120 GPa for LaC and LaN, respectively. Taking into account an argument used in Ref. 100 for VN, we can suggest elastic instability of $B1$ LaC and LaN, i.e., it might be that the crystalline structure of LaC and LaN is rather different from the $B1$ type.

IV. PHONON SPECTRA OF BCC METALS

In this section we present the calculated phonon spectra for the investigated bcc metals (V, Nb, Ta, Mo, and W) in order to illustrate the ability of the generated pseudopotentials. There are some common features for the spectra of the V^b group bcc metals [Figs. 2(a)–2(c)]. First of all, they have the same shape in the [100] and [111] directions. There is a dip of the LA mode along the [100] line near the H point $[q=(0.7,0.7,0)]$. Another observed dip near the P point $[q=(0.7,0.7,0.7)]$ and crossing of TA and LA modes at the P point. In these directions, due to the underlying bcc structure, the phonon spectra of Nb and Ta could be successively approximated by scaling the spectrum for V by a factor of $\sqrt{M_X/M_V}$ where M_X is the atomic mass of an atom X (X =Nb,Ta), and M_V is the atomic mass of V. Indeed, the calculated ratio is equal to 1.35, and 1.88 for Nb and Ta, respectively. The frequency ratio ω_V/ω_X is equal to 1.15 and 1.57 at the P point and for the H point the ratio of frequencies is 1.2 and 1.6, for Nb and Ta, correspondingly. So, the frequency ratio is practically the same for two characteristic points, and approximately equal to $\sqrt{M_X/M_V}$ confirming our suggestion. Another common feature for the spectra is the softening of the transversal acoustic (TA) mode for the long-range wave

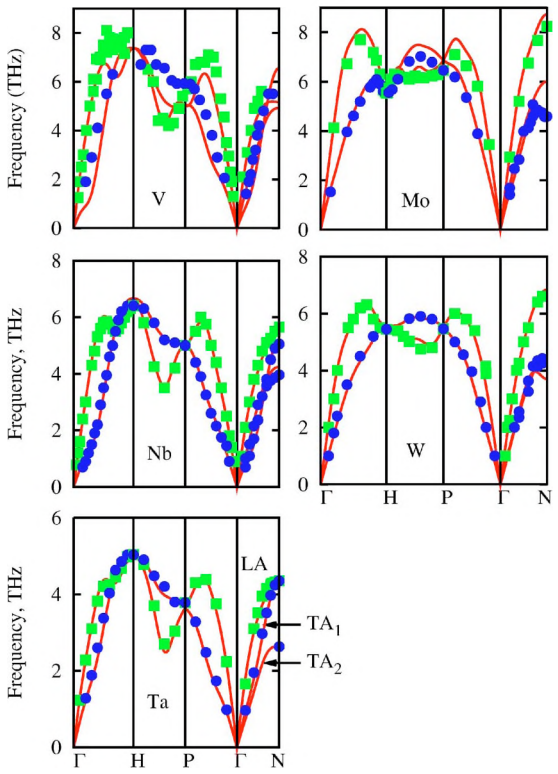

FIG. 2. (Color online) The phonon spectra of IV^b and V^b bcc metals along high symmetry directions in the Brillouin zone. In (a) the spectrum for V is depicted for which there is no available inelastic neutron scattering experiment results. The squares and circles are results of early TDS experiments (Ref. 112) and refer to the LA and TA modes, respectively. Experimental points for Nb (b), Ta (c), Mo (d), and W (e) are taken from (Refs. 108–111), respectively. Γ-*H*, *H*-*P*-Γ, and Γ-*N* refer to [100] [111], and [110] directions, respectively. TA_2 mode corresponds to the lowest mode along the Γ-*H* direction near the Γ point, LA is the highest mode, and TA_1 mode lies between these two modes at the same *q* point. These modes are specified for Ta.

vectors. This is more pronounced for Nb for which the superconducting temperature (9.25 K) is the highest among the elemental metals at ambient conditions.

A difference between the spectra appears in the [110] direction. One can see that at the *N* point the TA_1 mode of V is higher than the TA_2 and the LA modes, and the crossing of the TA_1 mode with both the TA_2 and LA modes takes place. For Nb the TA_1 has a crossing point with only the TA_2 mode. Finally, for Ta the TA_2 and LA modes are approximately degenerated and there is no crossing of the modes in the [110] direction.

The phonon spectra of VI^b group metals Mo [Fig. 2(d)] and W [Fig. 2(e)] do not have features which are presented by V^b group bcc metals. Mo and W have pronounced softening of the LA mode near the *H* point. Near the *N* point softening of the transversal mode takes place for both metals. The main difference in the phonon spectrum of Mo and W is the appearance of crossing LA and TA modes near the *H* point along the high symmetry [111] direction.

A comparison between the calculated and experimental results shows a very good agreement between *ab initio* lattice dynamics and inelastic neutron scattering experiments[108–111] for Nb, Ta, Mo, and W. The agreement with recent FP-LMTO calculations in Ref. 48 is also very good for V, Nb, and Ta (see Table IV), and for W there is good agreement with norm-conserving pseudopotential calculations of Refs. 86 and 93. For V inelastic neutron scattering measurements of the phonon spectrum are not available and the accuracy of the x-ray thermal diffuse scattering (TDS) method seems to be low,[112] though recently it has been demonstrated that the accuracy of the TDS method can be enhanced considerably, and as a result good agreement with the neutron experiments for Nb was obtained.[113]

TABLE IV. Comparison of calculated phonon frequencies for bcc metals in high symmetry *H* and *N* points (in THz).

		V	Nb[a]	Ta[b]	Mo[c]	W[d]
H_{LT}	Theor.[e]	7.95	6.67	4.99	5.57	5.57
	Theor.[f]	8.03	6.43	5.13	5.71	
	Expt.		6.49	5.03	5.52	5.50
N_L	Theor.[e]	7.04	5.58	4.35	8.72	3.70
	Theor.[f]	7.22	5.52	4.53	7.99	
	Expt.		5.66	4.35	8.14	
N_{T1}	Theor.[e]	5.35	4.25	2.64	6.00	4.54
	Theor.[f]	4.76	3.94	2.65	5.74	
	Expt.		3.93	2.63	5.73	4.50
N_{T2}	Theor.[e]	5.98	5.19	4.24	4.67	6.75
	Theor.[f]	6.17	4.80	4.18	4.69	
	Expt.		5.07	4.35	4.56	6.80

[a]Reference 108.
[b]Reference 109.
[c]Reference 110.
[d]Reference 111.
[e]This work.
[f]Reference 48.

V. DESCRIPTION OF PHONON SPECTRA OF TMC AND TMN

First, we consider the phonon dispersion relations in carbides and nitrides of Sc and Y [Fig. 3(a)–3(d)], the III^b group metals. They show common features, but there are also some differences in the spectra. For instance, for ScC and YC the frequency of the TA_2 mode in the [110] direction is higher compared to the one for the longitudinal mode. A difference between the spectra of ScC and YC is that there is an overlap between optical and acoustical modes in ScC, but in the case of YC the modes are separated by a frequency gap of 0.77 THz.

The shapes of the acoustic branches of ScN and YN [Figs. 3(c) and 3(d)] are typical for the fcc based structure and do not contain any peculiarities. Despite a substansital difference of the atomic mass between the metal and nonmetal atoms, the optical and acoustic modes are not separated, as it can be expected. The main difference between the spectra of ScN and YN and other TM carbides and nitrides is a splitting of the LO and transversal TO modes at the Γ point which is characteristic for polar semiconductors and insulators, and is due to nonuniformly distributed charge density. Based on this observation we suggest that ScN and YN are semiconductors. Indeed, like $A^{III}B^{V}$ semiconductors, ScN and YN have eight electrons per unit cell which are expected

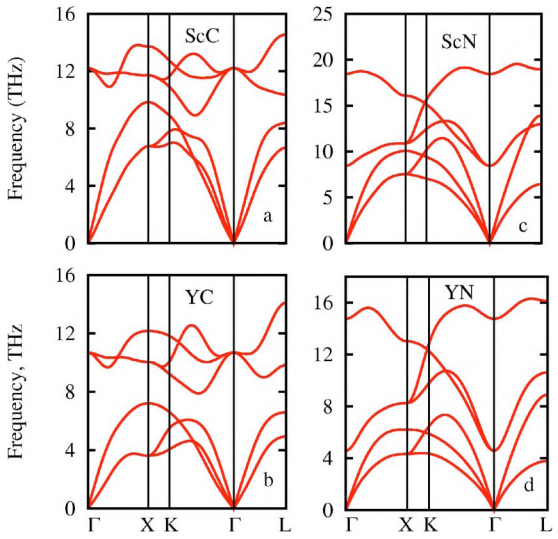

FIG. 3. (Color online) The phonon spectra of III^b group metal carbides and nitrides along high symmetry directions in the Brillouin zone: (a) ScC, (b) ScN, (c) YC, and (d) YN. No experimental data available for stoichiometric III^b group metal carbides and nitrides. Γ-*X*, *X*-*K*-Γ, and Γ-*L* correspond to the [100] [110], and [111] high symmetry directions, respectively..

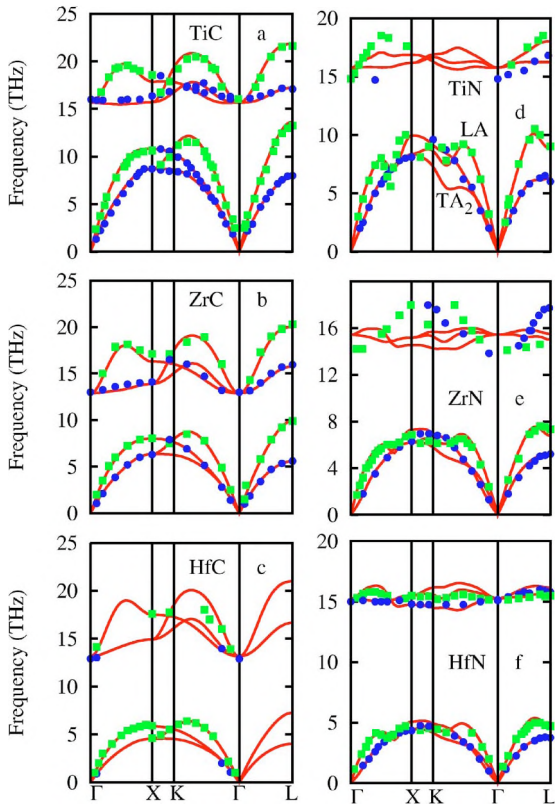

FIG. 4. (Color online) Phonon dispersion curves for IV^b group metal carbides and nitrides along high symmetry directions in the Brillouin zone. Experimental points for TiC (a), TiN (b), ZrC (c), ZrN (d), HfC (e), and HfN (f) are taken from Refs. 39, 52, 41, 53, 36, and 54, respectively. The circles and squares refer to the transversal and longitudinal modes for both acoustic and optical brances. Note the reverse order for LO and TO modes for HfN and ZrN.

to be paired leading to covalentlike bonding. Our suggestion is in agreement with result of recent optical measurements,[114] and exact-exchange (EXX) calculations,[114] as well as with screened-exchange (S-X) calculations[17] where the experimental and the S-X band gap, E_g, for ScN was found to be 1.3 eV, but somewhat overestimated in EXX calculations, 1.6 eV. The gap for YN is much smaller and is 0.85 eV.[17]

The calculated microscopic dielectric constants are 12.9 and 12.5 for ScN and YN, respectively, and they seem to be reasonable. For example, $\epsilon(0)=12.9$ for GaAs ($E_g=1.42$ eV) and $\epsilon(0)=15.7$ for GaSb ($E_g=0.726$ eV). Taking into account the fact that $\epsilon(0)$ becomes lower for larger E_g, we suggest that E_g for YN is underestimated in S-X calculations. Calculated effective charges, Z^*, for ScN and YN are $\pm 4.3e$.

It is also interesting to check the Laddyne-Saks-Teller (LST) law $\epsilon_\infty/\epsilon(0)=\omega_{LO}^2/\omega_{TO}^2$ for optical modes. Unfortunately, we are not aware about ϵ_∞, either for ScN or YN. Nevertheless, we estimated $\epsilon(0)/\epsilon_\infty$ for a wide range of ionic crystals[87] and $A^{III}B^{V}$ semiconductors and found that the ratio varied in the range of 1–6. Our calculated value $\omega_{LO}^2/\omega_{TO}^2$ for ScN at the Γ point is about 5, but for YN the ratio is two times larger and is about 10.5. Taking into account the calculated dielectric constant for the low frequency limit, we estimated ϵ_∞ for YN to be ~1.4 instead of 2.6 for ScN. So, unlike conventional semiconductors with small band gap, the estimated values for ϵ_∞ in ScN and YN are very low. Owing to the low ϵ_∞, YN appears as a promising material for high frequency applications. The phonon spectra of ScN and YN were not studied experimentally and due to this circumstance the calculated spectra should be considered as a prediction.

The calculated spectra for the IV^b group metal carbides are presented in Figs. 4(a)–4(c) where they are compared with available experimental data, and additionally, we compare calculated frequencies at high symmetry Γ, *X*, and *L* points for TiC (Table V) with experimental [39] and theoretical [50] results. We notice the excellent agreement between the theoretical and experimental results for the carbides. The acoustic branches do not possess any peculiarities and are similar to those for noble metals with fcc lattice which are not superconducting materials. As it was mentioned in Ref. 39, acoustic modes in TiC are not sensitive to the presence of carbon vacancies, in contrast to the case of superconducting NbC. Indeed, phonon dispersion curves for TiC containing 5% and 11% vacancies in the carbon sublattice are practically the same.[39] The difference between optical branches which are mainly affected by nonstoichiometry is about 3.5% for different carbon vacancy concentrations.

In contrast to carbides, the acoustic branches of mononitrides [Figs. 4(d)–4(f) show anomalies in [100], [110], and [111] directions. There is a dip of the longitudinal acoustic

TABLE V. Comparison of calculated phonon frequencies of TiC in high symmetry points Γ, *X*, and *L* (in THz).

	Γ_{LTO}	X_{TA}	X_{LA}	X_{TO}	X_{LO}	L_{TA}	L_{LA}	L_{TO}	L_{LO}
Theor.[a]	15.6	8.75	10.8	15.6	17.7	7.9	13.6	17.1	21.66
Theor.[b]	15.6	8.50	10.7	15.3	17.7				
Expt.[c]	16.3	8.50	10.8	16.5	18.5	8.07	13.35	17.08	21.58

[a]This work.
[b]Reference 50.
[c]Reference 39.

mode along the [100] direction (near $q \approx 0.7$) and a softening of both the longitudinal and transversal acoustic modes along the direction [110]. For TiN a pronounced softening of the LA mode near the L point also takes place, but the softening for ZrN and HfN is rather weak compared to TiN in accordance with experimental results.[52–54] It should also be noted that the softening is less pronounced for metals with larger atomic number. Besides, we note that the experimental depth of the dip for the LA mode of TiN is larger than the calculated one. Our experience allows us to suggest that a more fine q mesh is required to reveal this peculiarity.

The TO and LO modes along the [111] direction for HfN are placed in inverse order, i.e., TO modes have higher frequencies than the LO mode, in accordance with the experimental observation[54] and, thus, confirming both the ability of DFPT and the good quality of the generated Hf pseudopotential. It should also be noticed that the behavior means that long-range Coulomb interactions are not screened by the conduction electrons which usually leads to the LST splitting of optic modes. This kind of unusual behavior of the optical modes is not caused by the crystal structure and has been observed, besides HfN, only in uranium carbide (UC) and uranium nitride (UN) in $B1$ structure. Analyzing our calculated spectrum, we have found that the reverse order in the LO and TO modes also takes place in ZrN, but not in TiN. Such behavior of the phonon modes in ZrN has not been reported prior to this work. The crossing of TO and LO optical modes in TiN holds near the K point whereas for ZrN and HfN it takes place near the (0.7,0,0) point in Γ-X direction. Comparison with the results of *ab initio* calculations[63] shows that optical modes are in somewhat worse agreement with experiments[53,54] when compared to the acoustic modes. While we also have poor agreement with optical modes for ZrN, our calculated optical modes of HfN are in good agreement with experimental data. In Ref. 63 the postion of the dip in the Δ direction for the TA_1 mode of HfN is noticeably shifted toward the X point as compared to experiments. Besides, the softening of the TA_1 mode of HfN along the Δ direction is more pronounced, but according to experimental results of Ref. 54 the softening is smeared out.

Presumably, the above mentioned features are responsible for superconductivity of TiN with a superconducting temperature of T_c=4.86 K (Ref. 23) or T_c=5.49 K.[2] Difference between the calculated and experimental phonon dispersion curves for optical modes for TiN is about 10% and is probably connected to the nonstoichiometry of the experimental sample[52] which contained 2% of the nitrogen vacancies. Spengler *et al.*[55] showed that the nonstoichiometry in the N sublattice was crucial for T_c. Indeed, they found that T_c=6.0 K for $TiN_{0.995}$, whereas for $TiN_{0.95}$ T_c is considerably reduced down to 1.7 K. We suggest that the changes in T_c are connected to changes of the phonon spectrum induced by N vacancies.

Acoustic and optical branches are separated by a frequency gap of around 2.5 THz for TiC and ZrC, but for HfC the gap is much larger, 6 THz. The band gaps between acoustic and optical branches are about 6, 7, and 10 THz for TiN, ZrN, and HfN, respectively. For the monocarbides of Ti, Zr, and Hf the gap is lower by approximately a factor of

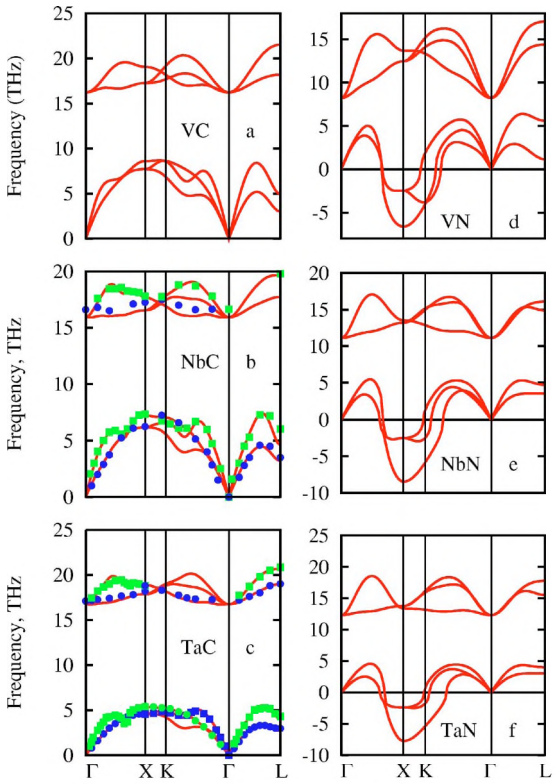

FIG. 5. (Color online) Phonon dispersion relations for V^b group metal carbides [(a)–(c)] and nitrides [(d)–(f)] along high symmetry directions in the Brillouin zone. For B1 VC (a) there are no experimental data. For NbC (b) and TaC (c) experimental points are from Refs. 36 and 34, correspondingly. The nitrides with ten valence electrons exhibit dynamical instability near the X point.

2. One can see that the band gap is increased when the period number is increased and the mass ratio M_X/M_{Me} is considerably reduced.

For V^b group metal monocarbides and mononitrides with the $B1$ structure we have found more exciting features. In contrast to the III^b and IV^b group metal carbides, the acoustic modes of V, Nb, and Ta monocarbides have anomalous features. In Fig. 5(a) we do not compare our calculated dispersion relations for VC with experiment, because VC is highly nonstoichiometric and there was no publication devoted to experimental synthesis and study of the stoichiometric VC.

For NbC [Fig. 5(b)] and TaC [Fig. 5(c)] we have found excellent agreement between the theoretical and experimental spectra (see also Table VI for NbC). The observed anomalies are a dip of LA modes in the [100] direction and a softening of both the LA and TA modes along the [110] and [111] directions. Compared to IV^b group metal mononitrides

TABLE VI. Comparison of calculated phonon frequencies for NbC in high symmetry Γ, X, and L points (in THz).

	Γ_{LTO}	X_{TA}	X_{LA}	X_{TO}	X_{LO}	L_{TA}	L_{LA}	L_{TO}	L_{LO}
Theor.[a]	15.9	6.12	7.15	16.4	17.54	3.3	4.8	17.6	19.50
Theor.[b]	17.05	6.37	7.51	17.64	18.65	4.26	6.02	18.82	21.60
Expt.[c]	16.70	6.35	7.30	17.20	17.80	4.00	6.00		19.20

[a]This work.
[b]Reference 48.
[c]Reference 36.

peculiarities of the spectra for VC, NbC, and TaC are not considerably suppressed upon increasing atomic number and a softening of the LA and TA modes near the L point is more pronounced. One should keep in mind that the monocarbides NbC and TaC are supercoductors with T_c=11, and 10 K, respectively.[2]

Neither VC nor VN were calculations compared to experiments because the experimental samples are highly nonstoichiometric and, so far, there was no report concerning the superconductivity of stoichiometric VC. The substoichometric $VC_{0.88}$ was found to be nonsuperconducting (T_c $<$0.05 K).[2] Besides, scattering cross section for V is completely incoherent which makes it difficult to conduct inelastic neutron scattering experiments for V-based alloys and compounds. Substoichiometric VN_x was studied in Ref. 56 and a pronounced softening of the acoustic modes near the X pointed was observed for $VN_{0.88}$. Nonorthogonal tight binding (NTB) method calculations for stoichiometric VN resulted in a very deep softening of the modes compared to experiments, and only the introduction of nitrogen vacancies has led to better agreement with experiment. Note that anomalies of the long-range force constants D_2 in VN are largely determined by nonmetal vacancies.

Introducing one more electron to a system results in a considerable change of the phonon spectra of V^b metal nitrides [Figs. 5(d)–5(f)]. We have found imaginary frequencies along the high symmetry $\Gamma-X$ direction, which is incompatible with the dynamic stability of VN, NbN, and TaN with the $B1$ structure. Therefore, the above mentioned mononitrides cannot be crystallized in the NaCl-type structure. In order to shed light on possible structure types for Nb mononitride we have considered two other structure types, namely, NiAs and WC. Results of phonon calculations for NbN within the NiAs and WC structures are presented in Figs. 6(a) and 6(b). One can see that the phonon spectrum of NbN in the NiAs-type structure [Fig. 6(a)] has an imaginary frequency near the M point. The calculated phonon dispersion relations for NbN with the WC structure [Fig. 6(b)] do not show any anomaly in any direction; therefore, NbN may adopt the WC-type structure. We have compared our conclusions to the results of the total energy calculations,[116] where NbN in the NaCl-, NiAs-, WC-, and NbO-type lattices have been considered. The last one is similar to the $B1$ structure where two atoms are removed from a corner and the center of a cubic cell. The results show that (see Figs. 1 and 3 in Ref. 116) the highest total energy corresponds to NbN with NbO-type structure (see also Ref. 117). Though the energy for the NaCl-type lattice is lower compared to NbO type, it is higher with respect to NiAs- and WC-type structures. The difference of the total energies for NiAs and WC types at equilibrium volume is about 0.013 eV/P.U., and the lowest total energy corresponds to the WC-type structure. Turning to Figs. 5(e) and 6(a), one can see that there is a high "degree" of instability of NbN in the NaCl type structure, but it is considerably reduced in the case of NiAs-type. The latter is a "nearly" stable lattice. The structure, presumably, could be stabilized by applying pressure.

Phonon dispersion relations of WC and WN have not been studied experimentally; nevertheless, we believe that

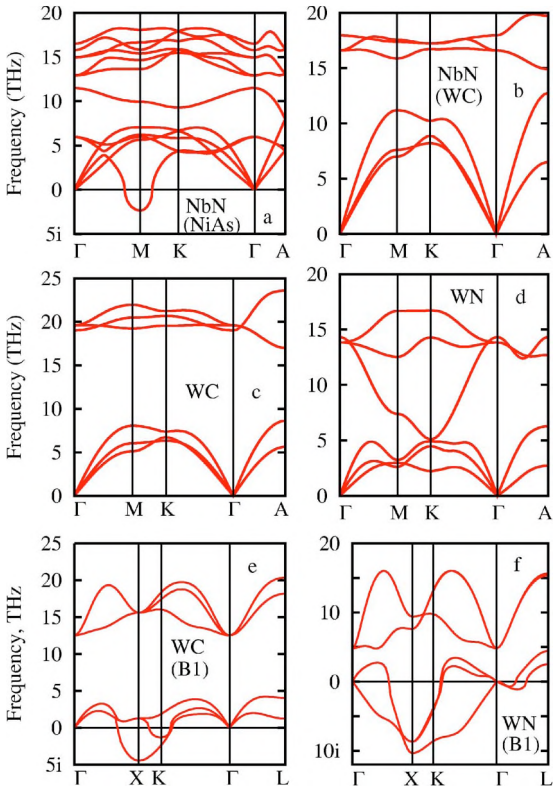

FIG. 6. (Color online) The phonon spectra for NbN within hexagonal NiAs- (a) and WC- (b) type structures along high symmetry directions in the Brillouin zone. The phonon spectra for hexagonal WC (c), WN (d), and WN (e) within cubic NaCl-type structure along high symmetry directions in the Brillouin zone are also presented.

the spectra for the WC-type structure [Figs. 6(c) and 6(d)] we have calculated are correct. There are no anomalies in the acoustic branches which could lead to an instability of hexagonal WC. A wide band gap between acoustic and optical modes is of about 9 THz. Compared to WC, the acoustic modes of WN have pronounced peculiarities along the [$\xi\xi$ 0] and [ξ 00] Γ-K-M-Γ directions [Fig. 6(d)]. High superconducting temperature (T_c=16 K) for $B1$ WN was predicted in Ref. 20, but we have shown that it is a dynamically unstable structure [see Fig. 6(f)]. We also note that the phonon spectrum for both WC and WN within WC-type structure resembles the spectrum for a cubic material, but not a hexagonal one. For the latter, the presence of almost linear TA and LA modes in the Γ-A direction is characteristic, see Γ-A direction in Fig. 6(a). The lack of this feature might be connected to c/a ratio which is close to 1 for the WC-type structure. Besides, it turned out that acoustic and optical modes of hexagonal WN are not separated by the large band gap, despite very large difference in atomic mass for W and N atoms. Similar behavior was revealed in studies using the norm-conserving pseudopotential for W. We suggest that it should be a subject for further investigations.

Let us now discuss the results of phonon calculations for MoC and MoN [Figs. 7(a)–7(c)]. The available investigations concerning the structure of MoC and MoN are controversial. The authors in Ref. 23 claimed that both MoC and MoN crystallize in the NaCl-type structure, and they have high T_c: 12.0 and 9.26 K for MoN and MoC, respectively.

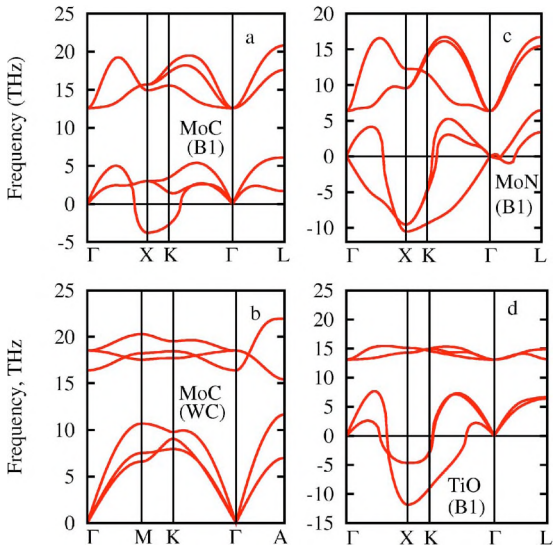

FIG. 7. (Color online) The phonon spectrum for $B1$ MoC (a), $B1$ MoN (b), and MoC within hexagonal WC- type (c) structure, and $B1$ TiO (d) along high symmetry directions in the Brillouin zone.

Recently this conclusion was questioned in Ref. 64. It turned out that MoC and MoN were never synthesized experimentally. In order to shed light on this failure we analyzed the phonon spectra. As can be seen from Figs. 7(a) and 7(c), the spectra for MoC and MoN in the NaCl-type structure exhibit imaginary frequencies. Therefore, they are dynamically unstable and this explains the experimental failure to produce $B1$-type MoC and MoN. Based on our phonon calculations [Fig. 7(b)] we have shown that MoC can crystallize in the WC-type structure in accordance with recent total energy calculations of Hugosson *et al.*[115] Unfortunately, neither of the structures considered in the present study was found to be dynamically stable for MoN.

VI. DISCUSSION

Let us now analyze our results in a somewhat different manner: namely, "from left to right" in the framework of the same period of the Periodic Table adding one more electron to a system rather than "up to down," i.e., for groups with isoelectronic atomic configuration. For this purpose we mapped the Periodic Table (see Tables VIIa and Table VIIb), on TMC and TMN, respectively. From these tables one can see that the total number of valence electrons in the system changes from 7 to 11, depending on whether we consider TMC or TMN. Blue and green columns indicate dynamically stable TMC or TMN, while TMC and TMN displayed in red columns means that they are dynamically unstable. Besides, green columns stand for superconducting carbides and nitrides.

Based on Tables VIIa and VIIb, we can formulate a general rule: if the monocarbides and mononitrides of the early transition metals with NaCl-type structure contain eight valence electrons, they are dynamically stable, and their acoustic modes do not contain any anomalies; if there are seven or nine electrons in the same system within the same structure, the acoustic modes have some peculiarities (softening of TA and LA modes), but the system is still dynamically stable. These peculiarities are the key factor for $B1$ TMC and TMN with seven or nine valence electrons in the unit cell to become superconducting. Monocarbides and mononitrides with ten and more electrons in the NaCl-type structure are dynamically unstable and a phase transformation to a dynamically stable phase should be expected. We have demonstrated this for NbN and MoC for which we have found that they should adopt the WC-type structure. The proposed rule was also tested for $B1$ TiO and ZrO, and it turned out that both these oxides are dynamically unstable, in agreement with their electron count, ten electrons in the unit cell. For example, in Fig. 7(d) we show result of our phonon calculations for TiO. The same conclusion for TiO was reached in Ref. 118 where the calculations were carried out by means of the linear response method in its FP-LMTO version.[48] It is very exciting that two very different compounds, such as TiO and MoC, demonstrate the same behavior due to their iso-

TABLE VII. (Color online) Tables illustrating dynamic stability boundary for TMC (a) and TMN (b) within $B1$ structure in dependence on N, the total number of valence electrons in the unit cell. The red columns stand for dynamically unstable TMC and TMN, and the green and blue columns refer to stable TMC and TMN. The green columns are for superconducting TMC and TMN.

a

	III^b	IV^b	V^b	VI^b
	Sc $3d^14s^2$	Ti $3d^24s^2$	V $3d^34s^2$	
	Y $4d^14s^2$	Zr $4d^24s^2$	Nb $4d^44s^1$	Mo $4d^54s^1$
		Hf $5d^24s^2$	Ta $5d^34s^2$	W $5d^44s^2$
N	7	8	9	10

b

	III^b	IV^b	V^b	VI^b
	Sc $3d^14s^2$	Ti $3d^24s^2$	V $3d^34s^2$	
	Y $4d^14s^2$	Zr $4d^24s^2$	Nb $4d^44s^1$	Mo $4d^54s^1$
		Hf $5d^24s^2$	Ta $5d^34s^2$	W $5d^44s^2$
N	8	9	10	11

electronic structure. So far Weber,[43] based on very limited number of experimental results, quoted that TaC and NbC, as well as TiN, ZrN, and HfN,[2,43] show significant phonon anomalies and the high T_c for ZrN is of about 10 K. The pseudobinary $NbC_{0.3}N_{0.7}$ and $NbN_{0.8}TiC_{0.2}$ systems with almost ten electrons have $T_c \sim 18$ K; however, they are unstable and undergo phase transitions.[2] We note that a high superconducting transition temperature is experimentally observed in systems with peculiarities in their acoustic modes and for systems with lattice instability.

The calculated electron-phonon interaction (EPI) constant λ for some carbides and nitrides, as well as for bcc metals, for which softening of acoustic modes takes place, are presented in Table VIII. It is easy to note that our calculated λ is in very good agreement with the EPI calculations of Savrasov[48] for pure bcc metals. Some difference between λ and $\omega_{\log}$ could be ascribed to different integration methods over the BZ. We used the weighted special point method, but in Ref. 48 the tetrahedron method was used. Zeller reported[61] the value λ=0.657 for Ta which is also in very good agreement with our calclulated λ. In Ref. 119 λ=0.88 was obtained using the rigid muffin-tin approximation (RMTA) for the calculation of the matrix elements of the electron-phonon interaction. This agrees well with other results presented in Table VIII, but λ=0.572 calculated using transport spectral function $\alpha_{tr}^2 F(\omega)$ seems to be somewhat low due to peculiarities in the real Fermi surface which enter via the group velocity of the electrons. Indeed, the backscattering of electrons from opposite sides of a nested Fermi surface will reduce λ by a factor $(1-v_k v_{k'}/|v_k|^2)$, where v_k is the group velocity of the electrons. Contrary, λ=1.05 given in Ref. 134 is higher by ~25% as compared to most of presented experimental, as well as theoretical results listed in Table VIII. Results from tunneling experiments give λ=0.69,[120,121] which is in excellent agreement with our value for λ=0.71 calculated fully from first principles.

Our electron-phonon interaction constants for TMC and TMN calculated from first principles are in excellent agreement with λ, calculated by other authors, see Table VIII, and evaluated from experimentally determined superconducting temperature using McMillan's equation[44] with a reliable Coulumb potential μ^*. In our calculations we used intermediate $\mu^* \approx 0.12$ if experimental information on T_c is absent; otherwise, we used μ^* which led us to better agreement with experimental superconducting temperature. It is interesting to note that the calculated λ for TMC and TMN vary within a narrow range of 0.59–0.67, and 0.78–0.87 for the nitrides and carbides, respectively, which, perhaps, reflects the similarity between their peculiarities in phonon dispersion relations. Indeed, the shape of the spectra for isoelectronic TMC and TMN with nine valence electrons in the unit cell is similar, and the observed difference could be ascribed to the presence of nonmetal vacancies and different atomic massess for TM. For example, a larger dip at $q \approx (0.7,0,0)$ is observed in $TiN_{0.98}$, but for HfN samples which contained up to 6% of nonmetal defects the dip along the [100] direction is considerably smeared out. Good agreement between our calculated EPI constants for the bcc metals, TMC, and TMN with experimental and theoretical EPI constants also confirm the high quality of the pseudopotentials we have generated. It is worth noting that nonstoichiometric $TiN_x(x=0.98)$ has a lower T_c (5.49 K), and as a result the evaluated λ is lower.[43,55] Moreover, for $x \leqslant 0.8$ TiN_x becomes nonsuperconducting at temperatures above 1.5 K.[55] Perfect or nearly perfect VC and VN samples were never reported to be superconducting experimentally. A reason for this is the very high chemical activity of V with respect to impurities, e.g., oxygen. Nevertheless, we predict that perfect stoichiometric $B1$ VC crystals should be superconducting with λ=0.78 and $T_c \sim 11.5$ K, respectively. Substoichiometric $VC_{0.88}$ was re-

TABLE VIII. Electron-phonon coupling constants and superconducting transition temperature for bcc metals, ScC and YC with seven valence electrons, and isoelectronic IV^b group metal nitrides and V^b group carbides with nine valence electrons in the unit cell. For each metal and compound in the first line we present results of our calculations, except μ, the Coloumb pseudopotential. Available experimental and theoretical data are shown in the next line.

	λ	μ	$\omega_{\log}$ (K)	T_c (K)
V	1.22	0.3	202	6.0
	1.19,[a] 0.82,[b] 1.00,[c] 1.17[c]	0.3[a]	245[a]	5.40[a]
Nb	1.22	0.15	124	9.4
	1.26,[a] 1.36,[d] 1.04,[c] 1.22[c] 0.9,[e] 1.17[c]	0.21[a]	185[a]	9.25[a]
Ta	0.71	0.12	148	4.6
	0.88,[f] 1.05,[g] 0.657,[h] 0.69[i,j] 0.86,[a] 0.572,[f] 0.78,[b] 0.83[c]	0.17,[a] 0.11[g,h]	160[a]	4.47[a]
TiN	0.59	0.145	470	6.0
	0.59,[k] 0.54[l]	0.13[k]		6.02,[k] 5.49[l]
ZrN	0.66	0.12	402	10.1
	0.622,[m] 0.672,[l] 0.6272,[n] 0.62[o]	0.11,[n] 0.1[m]		10.0[l]
HfN	0.67	0.115	323	8.9
	0.686,[m] 0.69,[l] 0.643[n]	0.11,[n] 0.1[m]		8.83[l]
VC	0.78	0.12	327	11.5
NbC	0.87	0.18	340	10.5
	0.66–0.72,[l] 0.63[p]			11.2[l]
TaC	0.78	0.12	272	10.4
	0.925,[k] 0.72[l]			10.6,[k] 10.35[l]
ScC	0.60	0.12	464	8.6
YC	0.76	0.12	375	13.6

[a]Reference 130.
[b]See (Refs. 3 and 39) in Ref. 130.
[c]Evaluated by Savrasovs from electronic specific-heat coefficient, Ref. 130.
[d]Reference 129.
[e]Reference 5 page 379.
[f]Reference 119.
[g]Reference 134.
[h]Reference 61.
[i]Reference 120.
[j]Reference 121.
[k]Reference 55.
[l]Reference 43.
[m]Reference 28.
[n]Reference 131.
[o]Reference 63.
[p]Reference 132.

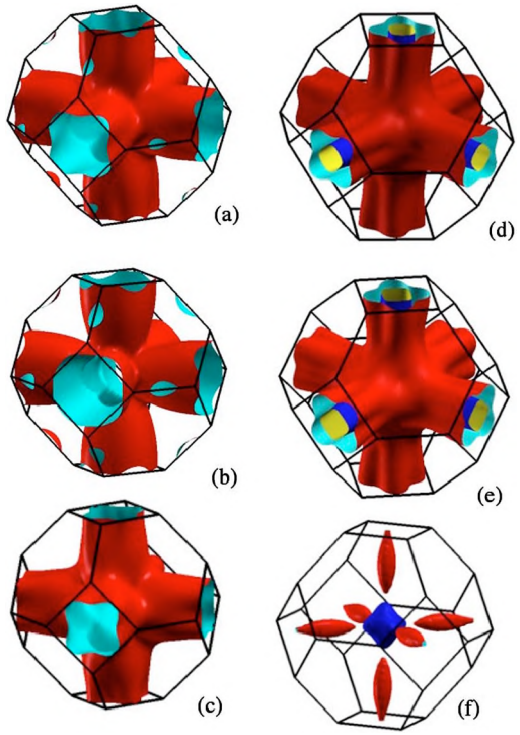

FIG. 8. (Color online) Fermi surface sheets for NbC (a), TiN (b), VC (c), ScC (d), YC (e), and TiC (f). FSs for ScC and YC look quite similar.

ported to be a nonsuperconducting material,[43] and, obviously, it tends to behave as its isoelectronic system TiN_x. It has also been shown theoretically[122] that N vacancies considerably decrease T_c of MoN_x ($x<1$) compared to that of the ideal $B1$ MoN, and this explains rather low T_c obtained experimentally.[123]

In addition, we have found that our calculated λ, 0.60, and 0.76 for ScC and YC, respectively, are comparable with those of conventional superconductors, and T_c evaluated from the Allen-Dynes equation using $\mu^*=0.12$ is 8.6 K for ScC and 13.6 K for YC.

The relation between phonon anomalies and peculiarities of the Fermi surface (FS) of Nb and NbC was discussed by Weber,[5] and it was found that for NbC wave vectors for which peculiarities in the phonon spectra were observed are connected to the Kohn anomalies, i.e., nesting of the FS sheets of NbC in these directions. Our calculated FS (Ref. 124) for NbC [Fig. 8(a)] is very similar to that shown in Ref. 5. Moreover, our calculated FSs for ScC [Fig. 8(b)], YC, VC [Fig. 8(c)], TaC, and TiN [Fig. 8(c)] show the same shape, and the latter FSs exhibit the same features as they have been found in the de Haas–van Alphen experiments and theoretical calculations by Haviland *et al.*[125] for TiN. Because of similarity of the FS to that for NbC for which a nesting situation of the FS sheets was observed we can suggest that the FSs for TMC and TMN with seven (ScC and YC) and nine valence electrons (VC, TaC, TiN, ZrN, and HfN) exhibit a nesting feature. One can easily observe the nesting situation for NbC [Fig. 9(a)] and VC [Fig. 9(b)], where contours of the inner electron sheet of the FS are parallel to the outer hole sheet of the FS. For VC the inner sheet of the FS formed by the electron bands exactly matches with the section of the

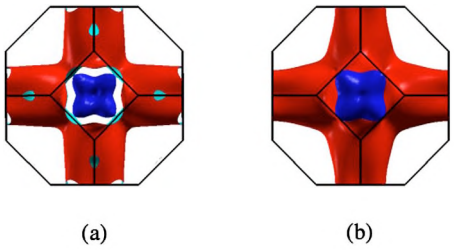

FIG. 9. (Color online) Illustration of the nesting behavior of the Fermi surface sheets for NbC (a) and VC (b).

tube along the [100] directions. At the same time, the FS for nonsuperconducting TiC with eight electrons [Fig. 8(e)] does not show the nesting behavior of the FS sheets. This observation is in agreement with the electron concentration rule, fundamental stability, and superconductivity in $B1$ compounds, formulated above. Vacancy induced changes in the FS may lead to the disappearence of the phonon spectra peculiarities followed by a quite sharp down of T_c.[126]

In Ref. 100 a drastic decrease of the C_{44} elastic constant for VN with ten valence electrons is observed and its low value, about 120 GPa, was interpreted as a precursor for an elastic instabilty. Moreover, MoN with 11 electrons in the unit cell was found[29,107] to be unstable with respect to orthorhombic and trigonal distorsions, and this is in agreement with our conclusion about lattice instability of $B1$-MoN. Wolf *et al.* studied a trend in formation and cohesion energy for some carbides and nitrides and concluded that MoN and CrN with 11 electrons do not crystallize in the NaCl structure. Due to this circumstance, the predicted high T_c in $B1$-MoN could not be observed in perfect stoichiometric MoN. We have found from our phonon dispersion curves that the elastic constants C_{44} and C' for VN, NbN, TaN, and MoC derived as a slope of the TA_2 mode along [100] and [110] directions must be positive. As a matter of fact, it is difficult to draw a conclusion about lattice instability of these compounds based only on elastic constants obtained from total energy calculations. Indeed, C_{44} for $B1$ MoC calculated by Hart and Klein[64] is positive, while for $B1$ MoN one can see that the slope of the TA mode is negative; thus, C_{44} is negative in agreement with Refs. 29, 64, and 107. Besides, Hart and Klein[64] showed that $B1$ MoN is elastically unstable even at high pressures, and suggested that there is an unstable phonon mode, which makes it impossible to synthesize $B1$ MoC experimentally. They gave a schematic picture of the phonon instability along the Γ-X direction. The longitudinal mode for NbC and MoC, given in Ref. 64, looks plausible, but according to the results of our calculation and the reported experimental conclusions on crystal structure of NbN, a mode for $B1$ NbN seems to be incorrect (see Fig. 4 of Ref. 64). Phillips[59] also suggested that there is a lattice instability in NaCl-type NbN. We would also like to note that recently possible high-pressure applications of OsC compounds have been discussed.[127] Taking into account the total number of valence electrons in $B1$ OsC, 12, and our preliminary phonon studies, we can conclude that $B1$ OsC is a dynamically unstable compound. This conclusion agrees with Refs. 101 and 127 according to which MoC and OsC crystallize in a hexagonal structure.

One of the main assumptions we have made in our phonon calculations is the harmonic approximation for the force constant calculations and, therefore, anharmonic terms are not taken into account in our calculations. Nevertheless, Weber *et al.*[42] noticed that anharmonic effects are small in TaC and NbC, because there is no noticeable difference in the phonon spectra measured at 4.2 and 300 K, but it was believed that the effects are important for $TaC_{1-x}N_x$ with $x \approx 0.4$, and NbN which seem to be unstable. Dodd *et al.*,[97] based on ultrasonic experiments for elastic and nonlinear acoustic properties, found that acoustic mode anharmonicity is small for TiC and TaC. Anharmonicity might stabilize the phonons for TiO, VN, and NbN near critical points, but it is unlikely to occur at sufficiently low temperatures giving large values of imaginary frequencies.

In conclusion, we have demonstrated that the linear response method in conjunction with the state-of-the-art ultrasoft pseudopotentials is able to reveal peculiarities of the phonon spectra for 3*d*, 4*d*, and 5*d* metals and their compounds. We have shown that superconductivity of some TM monocarbides and mononitrides is connected to peculiarities of the FS, and acoustic modes of the phonon spectrum. The superconducting temperature is higher in systems with more pronounced anomalies of acoustic modes. The calculated electron-phonon coupling constants for metals and compounds of interest are in very good agreement with available experimental and theoretical data. We have shown that the reason for the experimental failure to synthesize a number of stoichiometric TM carbides and nitrides in $B1$ structure is due to dynamic instability. Besides, we summarized that lattice stability of TM carbides and nitrides, as well as oxides, is strongly affected by the total number of valence electrons. The phonon spectra for a number of TMC and TMN are predicted and, thus, there is a challenge for experimentalists to synthesize these compounds and then carry out inelastic neutron scattering or x-Ray TDS measurements for phonon dispersion curves. We also predict that perfect ScC, YC, and VC crystals with $B1$ structure are dynamically stable, and should be rather good superconductors with $T_c \approx 8.6$, 13.6 and 11.5 K, respectively. Based on details of the phonon spectrum of $B1$ YN, we suggest that this compound is a semiconductor crystal.

ACKNOWLEDGMENTS

The authors are grateful to the Royal Swedish Academy (KVA) for supporting collaboration between Russian and Swedish scientists. Two of the authors (E.I.I. and Yu.Kh.V.) thank RFBR (05-02-17464 and 06-02-17542) and NWO (Grant No. 047.016.005) for financial support. Swedish Foundation for Strategic Research and Swedish Research Council are also acknowledged. One of the authors (E.I.I.) is indebted to D. Vanderbilt, A. Christensen, and J. Inigues for their help in the early stage of ultrasoft pseudopotential generation. Most of the calculations are performed on SARA supercomputer, Amsterdam, The Netherlands, and partially, on National Supercomputer Center, Linköping, Sweden.

[1] C. S. Barrett and T. B. Massalski, *Structure of Metals* (Pergamon, New York, 1980).
[2] L. E. Toth, *Transition Metal Carbides and Nitrides* (Academic, New York, 1971).
[3] E. K. Storms, *The Refractory Carbides* (Academic, New York, 1967).
[4] V. A. Gubanov, A. L. Ivanovsky, and V. P. Zhukov, *Electronic Structure of Refractory Carbides and Nitrides* (Cambridge University Press, Cambridge, 1994).
[5] W. Weber, in *The Electronic Structure of Complex Systems*, NATO ASI Series, Vol. 113, edited by P. Phariseau and W. M. Temmerman (Plenum, New York, 1995).
[6] A. Neckel, P. Rastl, R. Eibler, P. Weinberger, and K. Schwarz, J. Phys. C **9**, 579 (1976).
[7] H. Bilz, Z. Phys. **153**, 338 (1958).
[8] P. Blaha, J. Redinger, and K. Schwarz, Phys. Rev. B **31**, 2316 (1985).
[9] A. Delin, O. Eriksson, R. Ahuja, B. Johansson, M. S. S. Brooks, T. Gasche, S. Auluck, and J. M. Wills, Phys. Rev. B **54**, 1673 (1996).
[10] R. Ahuja, O. Eriksson, J. M. Wills, and B. Johansson, Phys. Rev. B **53**, 3072 (1996).
[11] K. Schwarz, J. Phys. C **8**, 809 (1975).
[12] D. J. Chadi and M. L. Cohen, Phys. Rev. B **10**, 496 (1974).
[13] T. Amriou, B. Bouhafs, H. Aourag, B. Khelifa, S. Bresson, and C. Mathieu, Physica B **325**, 46 (2003).
[14] L. F. Mattheiss, Phys. Rev. B **5**, 315 (1972).
[15] E. Ehrenfreund and T. H. Geballe, Phys. Rev. B **5**, 758 (1972).
[16] A. F. Guillermet, J. Häglund, and G. Grimvall, Phys. Rev. B **48**, 11673 (1993); **45**, 11557 (1992); J. Häglund, G. Grimvall, T. Jarborg, and A. F. Guillermet, *ibid.* **43**, 14400 (1991).
[17] C. Stampfl, W. Mannstadt, R. Asahi, and A. J. Freeman, Phys. Rev. B **63**, 155106 (2001).
[18] N. Takeuchi, Phys. Rev. B **65**, 045204 (2002).
[19] F. Vines, S. Sousa, P. Liu, J. A. Rodriguez, and F. Illas, J. Chem. Phys. **122**, 174709 (2005).
[20] D. A. Papaconstantopoulos, W. E. Pickett, B. M. Klein, and L. L. Boyer, Phys. Rev. B **31**, 752 (1985).
[21] D. A. Papaconstantopoulos, W. E. Pickett, B. M. Klein, and L. L. Boyer, Nature (London) **308**, 494 (1984).
[22] W. E. Pickett, B. M. Klein, and D. A. Papaconstantopoulos, Physica B & C **107**, 667 (1981).
[23] B. T. Matthias and J. K. Hulm, Phys. Rev. **87**, 799 (1952).
[24] T. H. Geballe, B. T. Matthias, J. P. Remeika, A. M. Glogston, V. B. Compton, J. P. Maita, and H. J. Williams, Physics (Long Island City, N.Y.) **2**, 293 (1966).
[25] J. Nagamatsu, N. Nakagawa, T. Muranaka, Y. Zenitani, and J. Akimitsu, Nature (London) **410**, 63 (2001).
[26] H. Rietschel, H. Winter, and W. Erichardt, Phys. Rev. B **22**, 4284 (1980).
[27] S. H. Jhi, S. G. Louie, M. L. Cohen, and J. Ihm, Phys. Rev. Lett. **86**, 3348 (2001).
[28] X.-J. Chen *et al.*, Proc. Natl. Acad. Sci. U.S.A. **102**, 3198 (2005).
[29] Z. Wu, X.-J. Chen, V. V. Struzhkin, and R. E. Cohen, Phys. Rev. B **71**, 214103 (2005).
[30] D. R. Hamann, X. Wu, K. M. Rabe, and D. Vanderbilt, Phys. Rev. B **71**, 035117 (2005).
[31] C. Stampfl and A. J. Freeman, Phys. Rev. B **67**, 064108 (2003).
[32] L. Yu, C. Stampfl, D. Marshall, T. Eshrich, V. Narayanan, J. M. Rowell, N. Newman, and A. J. Freeman, Phys. Rev. B **65**, 245110 (2002).
[33] H. W. Hugosson, O. Eriksson, L. Nordström, U. Jansson, L. Fast, A. Delin, J. M. Wills, and B. Johansson, J. Appl. Phys. **86**, 3758 (1999); H. W. Hugosson, L. Nordström, U. Jansson, B. Johansson, and O. Eriksson, Phys. Rev. B **60**, 15123 (2000); H. W. Hugosson, P. Korzhavyi, U. Jansson, B. Johansson, and O. Eriksson, *ibid.* **63**, 165116 (2001); H. W. Hugosson, U. Jansson, B. Johansson, and O. Eriksson, Chem. Phys. Lett. **333**, 444 (2001); H. W. Hugosson, O. Eriksson, U. Jansson, and B. Johansson, Phys. Rev. B **63**, 134108 (2001); P. Korzhavyi, L. V. Poiurovskii, H. W. Hugosson, and B. Johansson, Phys. Rev. Lett. **88**, 015505 (2002).
[34] H. G. Smith and W. Gläzer, Phys. Rev. Lett. **25**, 1611 (1970).
[35] H. G. Smith, Phys. Rev. Lett. **29**, 353 (1972).
[36] H. G. Smith and W. Gläzer, in *Proceedings of the International Conference on Phonons, Rennes, France, July 1971*, edited by M. A. Nusimovici (Flammaron Sciences, Paris, 1971).
[37] M. Mostoller, Phys. Rev. B **5**, 1260 (1972).
[38] V. Heine and I. Abarenkov, Philos. Mag. **9**, 451 (1964); I. Abarenkov and V. Heine, *ibid.* **12**, 529 (1965).
[39] L. Pintschovius, W. Reichardt, and B. Scheerer, J. Phys. C **11**, 1557 (1978).
[40] M. V. Klein, J. A. Holy, and W. S. Williams, Phys. Rev. B **17**, 1546

(1978).
[41]W. Weber, Phys. Rev. B **8**, 5082 (1973).
[42]W. Weber, H. Bilz, and U. Schröder, Phys. Rev. Lett. **28**, 600 (1972).
[43]W. Weber, Phys. Rev. B **8**, 5093 (1973).
[44]W. L. McMillan, Phys. Rev. **167**, 331 (1968).
[45]G. M. Eliashberg, Zh. Eksp. Teor. Fiz. **38**, 966 (1960) [Sov. Phys. JETP **11**, 696 (1960)].
[46]S. K. Sinha and B. N. Harmon, Phys. Rev. Lett. **35**, 1515 (1975).
[47]K. S. Upadhyaya, A. K. Singh, A. Pandey, S. N. Pathak, and A. K. Singh, Pramana, J. Phys. **64**, 299 (2005).
[48]S. Yu. Savrasov, Phys. Rev. B **54**, 16470 (1996).
[49]E. G. Maksimov, M. V. Magnitskaya, S. V. Ebert, and S. Yu. Savrasov, JETP Lett. **80**, 548 (2004).
[50]P. T. Jochym, K. Parlinski, and M. Sternik, Eur. Phys. J. B **10**, 9 (1999).
[51]P. T. Jochym, K. Parlinski, and M. Sternik, Eur. Phys. J. B **15**, 265 (2000).
[52]W. Kress, P. Roedhammer, H. Bilz, W. D. Teuchert, and A. N. Christensen, Phys. Rev. B **17**, 111 (1978).
[53]A. N. Christensen, O. W. Dietrich, W. Kress, and W. D. Teuchert, Phys. Rev. B **19**, 5699 (1979).
[54]A. N. Christensen, W. Kress, M. Miura, and N. Lehner, Phys. Rev. B **28**, 977 (1983).
[55]W. Spengler, R. Kaiser, A. N. Christensen, and G. Müller-Vogt, Phys. Rev. B **17**, 1095 (1978).
[56]W. Weber, P. Rödhammer, L. Pintschovius, W. Reichardt, F. Gompf, and A. N. Christensen, Phys. Rev. Lett. **43**, 868 (1979).
[57]N. Tralshawala, J. F. Zasadzinski, L. Coeffy, W. Gai, M. Romalis, Q. Huang, R. Vaglio, and K. E. Gray, Phys. Rev. B **51**, 3812 (1995).
[58]G. F. Hardy and J. K. Hulm, Phys. Rev. **93**, 1004 (1954); H.-T. Chiu and S.-H. Chuang, J. Mater. Res. **8**, 1353 (1993).
[59]J. C. Phillips, Phys. Rev. Lett. **26**, 543 (1971).
[60]H. Frölich, Phys. Lett. **35A**, 325 (1971).
[61]H. R. Zeller, Phys. Rev. B **5**, 1813 (1972).
[62]X.-J. Chen, V. V. Struzhkin, S. Kung, H.-K. Mao, R. J. Hemley, and A. N. Christensen, Phys. Rev. B **70**, 014501 (2004).
[63]R. Heid, K.-P. Bohnen, B. Renker, T. Wolf, and H. Schober, Phys. Rev. B **71**, 092302 (2005).
[64]G. L. W. Hart and B. M. Klein, Phys. Rev. B **61**, 3151 (2000).
[65]R. A. Bartynski, S. Yang, S. L. Hilbert, C.-C. Kao, M. Weinert, and D. M. Zehner, Phys. Rev. Lett. **68**, 2247 (1992); K. Edamoto, S. Maehama, E. Miyazaki, and H. Kato, Phys. Rev. B **39**, 7461 (1989); P. A. P. Lindberg, P. L. Wincott, L. I. Johansson, and A. N. Christensen, *ibid.* **36**, 4681 (1987).
[66]H. W. Hugosson, O. Eriksson, U. Jansson, A. V. Ruban, P. Souvatzis, and I. A. Abrikosov, Surf. Sci. **557**, 243 (2004); H. W. Hugosson, O. Eriksson, U. Jansson, and I. A. Abrikosov, *ibid.* **585**, 101 (2005); M. Marlo and V. Milman, Phys. Rev. B **62**, 2899 (2000); A. Vojvodic, C. Ruberto, and B. I. Lundqvist, Surf. Sci. **600**, 3619 (2006).
[67]H. Isida and K. Terakura, Phys. Rev. B **34**, 5719 (1986); C. Oshima, T. Aizawa, M. Wuttig, R. Souda, S. Otani, Y. Ishizawa, H. Ishida, and K. Terakura, *ibid.* **36**, 7510 (1987); H. Ishida and K. Terakura, *ibid.* **36**, 4403 (1987); C. Oshima, R. Souda, M. Aono, S. Otani, and Y. Ishizawa, Phys. Rev. Lett. **56**, 240 (1986); *ibid.* **52**, 1907 (1984).
[68]E. I. Isaev, R. Ahuja, S. I. Simak, A. I. Lichtenstein, Yu. Kh. Vekilov, B. Johansson, and I. A. Abrikosov, Phys. Rev. B **72**, 064515 (2005).
[69]B. X. Liu and X. Y. Cheng, J. Phys.: Condens. Matter **4**, L265 (1992).
[70]A. Filippetti, W. E. Pickett, and B. M. Klein, Phys. Rev. B **59**, 7043 (1999).
[71]P. S. Herle, M. S. Hegde, N. Y. Vasathacharya, S. Philip, M. V. Rama Rao, and T. Sripathi, J. Solid State Chem. **134**, 120 (1997).
[72]G. L. Olcese, J. Phys. F: Met. Phys. **9**, 566 (1979).
[73]P. Hohenberg and W. Kohn, Phys. Rev. **136**, B864 (1964).
[74]W. Kohn and L. J. Sham, Phys. Rev. **140**, A1133 (1965).
[75]D. Vanderbilt, Phys. Rev. B **41**, 7892 (1990).
[76]J. P. Perdew, K. Burke, and M. Ernzerhof, Phys. Rev. Lett. **77**, 3685 (1996).
[77]J. P. Perdew, Phys. Rev. B **33**, 8822 (1986); A. D. Becke, Phys. Rev. A **38**, 3098 (1988).
[78]S. G. Louie, S. Froyen, and M. L. Cohen, Phys. Rev. B **26**, 1738 (1982).
[79]X. W. Wang, B. N. Harmon, Y. Chen, K.-M. Ho, C. Stassis, and W. Weber, Phys. Rev. B **33**, 3851 (1986).
[80]H. J. Monkhorst and J. D. Pack, Phys. Rev. B **13**, 5188 (1976).
[81]M. Methfessel and A. Paxton, Phys. Rev. B **40**, 3616 (1989).
[82]S. Baroni, S. De Gironcoli, A. Dal Corso, and P. Giannozzii, Rev. Mod. Phys. **73**, 515 (2001).
[83]S. Baroni *et al.*, http://www.pwscf.org/
[84]P. B. Allen and R. C. Dynes, Phys. Rev. B **12**, 905 (1975).
[85]O. L. Anderson, *Equation of State of Solids for Geophysics and Ceramic Science* (Oxford University Press, Oxford, 1995).
[86]A. Debernardi, M. Alouani, and H. Dreyssé, Phys. Rev. B **63**, 064305 (2001).
[87]C. Kittel, *Introduction to Solid State Physics*, 6th ed. (Wiley, New York, 1986).
[88]K. A. GschneidnerJr., in *Solid State Physics*, edited by F. Seitz and D. Turnbull (Academic, New York, 1964), Vol. 16, pp. 275–426.
[89]Y. Zhao *et al.*, Phys. Rev. B **71**, 184119 (2005).
[90]E. Fawcett, Rev. Mod. Phys. **60**, 209 (1988).
[91]G. Bihlmayer, T. Asada, and S. Blügel, Phys. Rev. B **62**, R11937 (2000).
[92]D. M. Bylander and L. Kleinman, Phys. Rev. B **29**, 1534 (1984).
[93]G. J. Ackland, X. Huang, and K. Rabe, Phys. Rev. B **68**, 214104 (2003).
[94]V. P. Zhukov, V. A. Gubanov, O. Jepsen, N. E. Christensen, and O. K. Anderson, J. Phys. Chem. Solids **49**, 841 (1988).
[95]D. Price, B. Cooper, and J. M. Wills, Phys. Rev. B **46**, 11368 (1992).
[96]M. Guemmaz, A. Mosser, R. Ahuja, and B. Johansson, Solid State Commun. **110**, 299 (1999).
[97]S. P. Dodd, M. Cankurtaran, and B. James, J. Mater. Sci. **38**, 1107 (2003).
[98]D. J. Siegel, L. G. HectorJr., and J. B. Adams, Phys. Rev. B **67**, 092105 (2003).
[99]H. P. Liermann, A. K. Singh, B. Manoun, S. K. Saxena, V. B. Prakapenka, and G. Shen, Int. J. Refract. Met. Hard Mater. **22**, 129 (2004).
[100]W. Wolf, R. Podloucky, T. Antretter, and F. D. Fisher, Philos. Mag. B **79**, 839 (1999).
[101]J. C. Grossman, A. Mizel, M. Côté, M. L. Cohen, and S. G. Louie, Phys. Rev. B **60**, 6343 (1999).
[102]P. Villars and L. D. Calvet, *Pearson's Handbook of Crystallographic Data for Intermetallic Phases* (American Society for Metals, Metals Park, OH, 1985).
[103]S. Méçabih, N. Amrane, Z. Nabi, B. Abbar, and H. Aourag, Physica A **285**, 392 (2000).
[104]I. R. Shein and A. L. Ivanovskii, e-print arXiv:cond-mat/0312391; only its reduced version was published in Solid State Commun. **131**, 223 (2004).
[105]R. Chang and L. J. Graham, J. Appl. Phys. **37**, 3778 (1966).
[106]N. A. Dubrovinskaya, L. S. Dubrovinsky, S. K. Saxena, R. Ahuja, and B. Johansson, J. Alloys Compd. **289**, 24 (1999).
[107]J. Chen, L. L. Boyer, H. Krakauer, and M. J. Mehl, Phys. Rev. B **37**, 3295 (1988).
[108]B. M. Powell, P. Martel, and A. D. B. Woods, Phys. Rev. **171**, 727 (1968).
[109]A. D. B. Woods, Phys. Rev. **136**, A781 (1964).
[110]J. Zaretsky, C. Stassis, B. N. Harmon, K.-M. Ho, and C. L. Fu, Phys. Rev. B **28**, 697 (1983).
[111]*Numerical Data and Functional Relationships in Science and Technology*, Landolt-Börnstein, New Series, Group III, Vol. 13a, Pt. 7, edited by K.-H. Hellwege and J. L. Olsen (Springer-Verlag, Berlin, 1981).
[112]R. Colella and B. W. Batterman, Phys. Rev. B **1**, 3913 (1970).
[113]M. Holt, P. Czoshke, H. Hong, P. Zschack, H. K. Birnbaum, and T.-C. Chang, Phys. Rev. B **66**, 064303 (2002).
[114]D. Gall, M. Städele, K. Järrendahl, I. Petrov, P. Desjardins, R. T. Haasch, T.-Y. Lee, and J. E. Greene, Phys. Rev. B **63**, 125119 (2001).
[115]H. W. Hugosson, U. Jansson, B. Johansson, and O. Eriksson, Science **293**, 2434 (2001).
[116]S. Ögut and K. M. Rabe, Phys. Rev. B **52**, 8585 (1995).
[117]E. C. Ethridge, S. C. Erwin, and W. E. Pickett, Phys. Rev. B **52**, R8589 (1995).
[118]P. A. Korzhavyi (unpublished).
[119]A. Al-Lehaibi, J. C. Swihart, W. H. Batler, and F. J. Pinski, Phys. Rev. B **36**, 4103 (1987).
[120]L. Y. L. Shen, Phys. Rev. Lett. **24**, 1104 (1970).
[121]E. L. Wolf, R. J. Noer, D. Burnell, Z. G. Khim, and G. B. Arnold, J. Phys. F: Met. Phys. **11**, L23 (1981).
[122]D. A. Papaconstantopoulos and W. E. Pickett, Phys. Rev. B **31**, 7093 (1985).
[123]G. Linker, R. Smithly, and O. Meyer, J. Phys. F: Met. Phys. **14**, L115 (1984).
[124]Fermi surface constructions are done using the XCRYSDEN package developed by A. Kokalj, see http://www.xcrysden.org; Comput. Mater. Sci. **28**, 155 (2003); the interface for the Quantum ESPRESSO code is written by E. I. Isaev.

[125] D. Haviland, X. Yang, K. Winzer, J. Noffke, and H. Eckardt, J. Phys. C **18**, 2859 (1985).
[126] W. E. Pickett, B. M. Klein, and R. Zeller, Phys. Rev. B **34**, 2517 (1986).
[127] J.-C. Zheng, Phys. Rev. B **72**, 052105 (2005).
[128] A. N. Christensen, O. W. Dietrich, W. Kress, W. D. Teuchert, and R. Currat, Solid State Commun. **31**, 795 (1979).
[129] J. S. Tse, Z. Li, K. Ueharo, Y. Ma, and R. Ahuja, Phys. Rev. B **69**, 132101 (2004).
[130] S. Yu. Savrasov and D. Yu. Savrasov, Phys. Rev. B **54**, 16487 (1996).
[131] P. Roedhammer, E. Gmelin, W. Weber, and J. P. Remeika, Phys. Rev. B **15**, 711 (1977).
[132] J. Greek, G. Linker, and R. Smithey, Phys. Rev. Lett. **57**, 3284 (1986).
[133] J. O. Kim, J. D. Achenbach, P. B. Mirkarimi, N. Shinn, and S. A. Barnett, J. Appl. Phys. **72**, 1805 (1992).
[134] L. L. Boyer, B. M. Klein, and D. A. Papaconstantopoulos, Ferroelectrics **16**, 201 (1977).
[135] H.-T. Chiu and S.-H. Chuang, J. Mater. Res. **8**, 1353 (1993).
[136] T. Mashimo, S. Tashiro, T. Toya, M. Nishida, H. Yamazaki, S. Yamaya, K. Oh-Ishi, and Y. Syono, J. Mater. Sci. **28**, 3349 (1993).
[137] B. X. Liu and X. Y. Cheng, J. Phys.: Condens. Matter **4**, L265 (1992).
[138] H. P. Lierman, A. K. Singh, B. Manon, S. K. Saxena, and C. S. Zha, Int. J. Refract. Met. Hard Mater. **23**, 109 (2005).
[139] D. J. Singh and B. M. Klein, Phys. Rev. B **46**, 14969 (1992).
[140] F. H. Featherstone and J. R. Neighbors, Phys. Rev. **130**, 1324 (1963).
[141] A. M. Nartowski, I. P. Parkin, M. MacKenzie, A. J. Craven, and I. MacLeod, J. Mater. Chem. **9**, 1275 (1999).
[142] X. Sha and R. E. Cohen, http://arxiv.org/pdf/cond-mat/0612338
[143] L. A. Salguero, L. Mancera, J. A. Rodrguez, and N. Takeuchi, Phys. Status Solidi B **243**, 1808 (2006).
[144] D. Gall, I. Petrov, N. Hellgren, L. Hulman, J. E. Sundgren, and J. Geene, J. Appl. Phys. **84**, 6034 (1998).
[145] L. L. Torre, B. Winkler, J. Schreuer, K. Knorr, and M. Avalos-Borja, Solid State Commun. **134**, 245 (2005).